Commun Nonlinear Sci Numer Simulat 161 (2026) 110013

Contents lists available at ScienceDirect

Communications in Nonlinear Science
and Numerical Simulation

journal homepage: www.elsevier.com/locate/cnsns

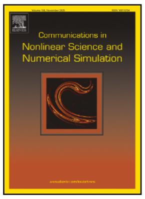

Research paper

Study of a nonlinear delayed parabolic model for prion disease dynamics with the unfolded protein response

Gangadhara Boregowda [a,*], Laurent Pujo-Menjouet [b], Zhaosheng Feng [a],
Michael R. Lindstrom [a]

[a] *School of Mathematical and Statistical Sciences, The University of Texas Rio Grande Valley, Edinburg 78539, Texas, USA*
[b] *Department of Mathematics, Université Claude Bernard Lyon 1, CNRS, Centrale de Lyon, INSA Lyon, Université Jean Monnet, ICJ UMR5208, Inria, Villeurbanne 69622, France*

ARTICLE INFO

Keywords:
Well-posedness
Prion
Reaction-diffusion equation
Nonlinear PDE
Upper and lower solution
Asymptotic stability

ABSTRACT

Prion diseases are neurodegenerative disorders characterized by the dynamic spread of misfolded toxic proteins in the brain. In this process, the normal cellular prion protein ($\mathrm{PrP^C}$) produced by neurons misfolds into a toxic form known as scrapie prion protein ($\mathrm{PrP^{Sc}}$). These misfolded proteins propagate through the brain by converting healthy prions into their toxic form. This biological mechanism can be modeled by a system of nonlinear parabolic partial differential equations, accompanied by a nonlinear delayed integral boundary condition. Our primary objective is to establish the existence of nonnegative classical solutions to this system. Furthermore, we derive a priori estimates for the total concentrations of $\mathrm{PrP^C}$ and $\mathrm{PrP^{Sc}}$ in the brain. Finally, we present numerical simulations to illustrate the spatiotemporal evolution of $\mathrm{PrP^C}$ and $\mathrm{PrP^{Sc}}$ and to capture oscillations in their concentrations.

1. Introduction

In recent years, mathematical models have played a critical role in understanding biological systems (see, for instance, [1,2]). In particular, neurodegenerative diseases (NDs), such as Alzheimer's disease (AD), Parkinson's disease (PD), and prion diseases, have been studied using network diffusion models and reaction-diffusion-based continuum models [3–5].

During the progression of prion diseases, the pathogenic scrapie prion protein ($\mathrm{PrP^{Sc}}$) present in the extracellular environment interacts with the normal cellular prion protein ($\mathrm{PrP^C}$) produced by neurons. This interaction promotes a conformational transformation of $\mathrm{PrP^C}$ into its misfolded, disease-associated counterpart, $\mathrm{PrP^{Sc}}$. This process leads to the accumulation of misfolded prions and their subsequent spread throughout the brain, resulting in neuronal dysfunction and ultimately cell death [6,7]. Elevated levels of $\mathrm{PrP^{Sc}}$ activate the Unfolded Protein Response (UPR), causing a temporary reduction in protein synthesis and thereby limiting the production of $\mathrm{PrP^C}$[8]. This adaptive cellular mechanism aims to minimize the accumulation of misfolded proteins and supports the clearance of toxic aggregates, enabling neurons to restore their normal activity. Sustained or excessive activation of the UPR may trigger signaling pathways that ultimately lead to programmed cell death [9]. Mathematically, this biological mechanism gives raise to a coupled system of non-linear reaction-diffusion equations with a delayed non-linear boundary condition.

In differential equation-based modeling, establishing the existence of a physically meaningful solution is both challenging and essential. However, in engineering applications, models are frequently investigated numerically under the assumption that a solution exists within a well-defined functional space; for instance, see books addressing numerical schemes for different classes of PDEs [10,

---

[*] Corresponding author.
E-mail address: gangadhara.boregowda@utrgv.edu (G. Boregowda).

https://doi.org/10.1016/j.cnsns.2026.110013
Received 25 January 2026; Received in revised form 20 March 2026; Accepted 6 April 2026

11]. Recently, reaction-diffusion equations with nonlinear boundary conditions have attracted considerable attention, with various theoretical aspects extensively studied in [12–14]. The existence of solutions for nonlinear delayed differential equations has also been addressed in the mathematical literature [15–18]. Notably, the framework of abstract parabolic equations in Banach spaces has proven to be a powerful tool for analyzing such systems [16,19]. Pao made significant contributions to the theory of nonlinear parabolic and elliptic equations by employing the method of upper and lower solutions, as documented in several of his works [15,20,21].

Building on the existing literature [20], this paper investigates a novel class of differential equations characterized by nonlinear, time-delayed boundary conditions. The primary focus is on establishing the existence of a unique, nonnegative classical solution to the proposed model and finding estimates on the solution. In addition, the study presents numerical simulations and visualizations of the solution, carried out using finite elements.

The structure of the paper is as follows: Section 2 presents the derivation and nondimensionalization of the mathematical model. Section 3 establishes the existence and uniqueness of a nonnegative solution. In Section 4, we derive useful estimates of the solution and discuss the biological implication. In Section 5, we establish asymptotic behavior of the proteins. Finite element solutions are presented in Section 6. Finally, Section 7 provides the conclusion and outlines the direction for future work. Additional supporting definitions and notations are included in Appendix A.

2. Material and methods

Our model considers a finite number ($N \geq 1$) of disjoint neurons, with the dynamics occurring in the surrounding interstitial fluid. Prion proteins exist in both membrane-bound and extracellular forms [22], but in this study we focus on the extracellular form to construct a simplified model. As such, we assume that cellular prion proteins are produced within neurons and released through the membrane into the intercellular space. Within the interstitial fluid, $\mathrm{PrP^C}$ can undergo spontaneous conformational misfolding into the pathogenic scrapie isoform, $\mathrm{PrP^{Sc}}$, at a rate $d \geq 0$. In addition, $\mathrm{PrP^{Sc}}$ can catalyze the conversion of $\mathrm{PrP^C}$ into $\mathrm{PrP^{Sc}}$ at a rate $c \geq 0$. Both $\mathrm{PrP^C}$ and $\mathrm{PrP^{Sc}}$ are cleared from the interstitial fluid at rates $a \geq 0$ and $b \geq 0$, respectively. We set up our system so that the local concentration of $\mathrm{PrP^{Sc}}$ near the neuronal membrane can trigger the UPR, with an approximate activation threshold S_c, leading to a reduction in the production of $\mathrm{PrP^C}$ from its maximum flux A [23]. The time for the UPR to active is modeled with a delay $t_d \geq 0$. The heterodimer dynamics of the proteins in the brain are schematically illustrated in Fig. 1. For simplicity, higher-order oligomers and aggregates are not included in this model.

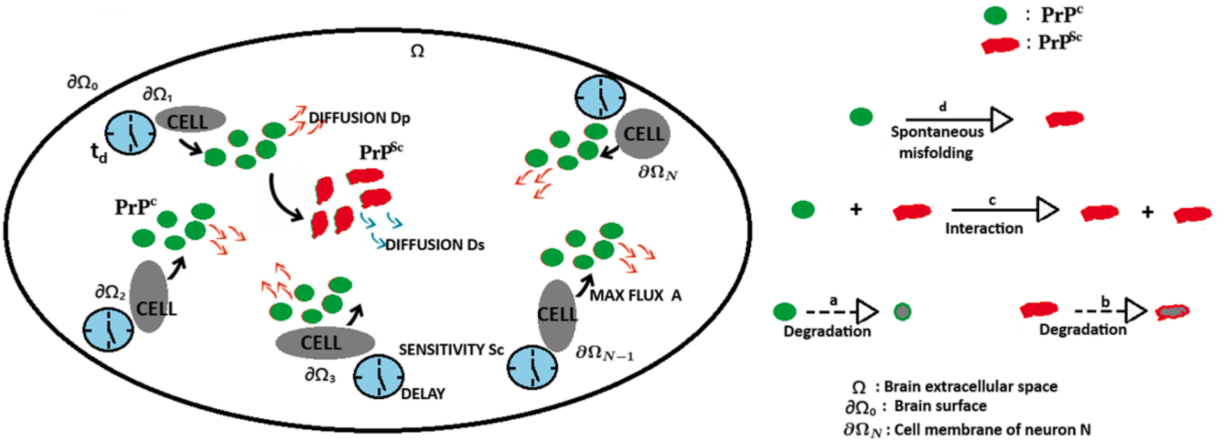

Fig. 1. Representative sketch of the model. Left: $\mathrm{PrP^C}$ is produced in the neurons and released into the intercellular space, where it diffuses with a rate D_P. $\mathrm{PrP^C}$ may be recruited to become $\mathrm{PrP^{Sc}}$, which diffuses at a rate D_S. The cell is sensitive to $\mathrm{PrP^{Sc}}$ at a concentration S_c and will reduce the maximum flux of $\mathrm{PrP^C}$ from A. Right: Spontaneous misfolding of $\mathrm{PrP^C}$ into $\mathrm{PrP^{Sc}}$ occurs at a rate d, conversion of $\mathrm{PrP^C}$ upon interaction with $\mathrm{PrP^{Sc}}$ occurs at a rate c, and the degradation rates for $\mathrm{PrP^C}$ and $\mathrm{PrP^{Sc}}$ are a and b, respectively.

2.1. Mathematical model

Neurons are physically small, bounded, three-dimensional structures in the human brain. Let N denote the total number of neurons, and let Ω_i represent an open, bounded, and connected domain in $\mathbb{R}^3$ corresponding to the i^{th} neuron, where $i = 1, 2, 3, \ldots, N$. We assume that the neuron domains are disjoint, i.e.,

$$\overline{\Omega}_i \cap \overline{\Omega}_j = \emptyset \quad \text{for } i, j = 1, 2, 3, \ldots, N, \text{ and } i \neq j.$$

The boundary $\partial\Omega_i$ represents the smooth cell membrane of the cell Ω_i. We consider the brain as an open bounded domain $\Omega_0 \subset \mathbb{R}^3$ with boundary $\partial\Omega_0$. We focus on the spread of proteins in the extracellular space in the brain, which leads to the computational domain as $\Omega = \Omega_0 \setminus \bigcup_{i=1}^{N} \overline{\Omega}_i$ with boundary $\partial\Omega = \bigcup_{i=0}^{N} \{\partial\Omega_i\}$. Let $P(x,t)$ and $S(x,t)$ denote the concentration of the PrP$^{\mathrm{C}}$ and PrP$^{\mathrm{Sc}}$, respectively, at position $x \in \overline{\Omega}$ and time $t \in [0,\infty)$. The dynamics of protein spreading in the extracellular space for $t > 0$ are given by

$$\frac{\partial P}{\partial t} = \overbrace{D_P \triangle P}^{\text{diffusion}} - \overbrace{cPS}^{\text{recruitment loss}} - \overbrace{dP}^{\text{spontaneous misfolding}} - \overbrace{aP}^{\text{degradation}}, \tag{1}$$

$$\frac{\partial S}{\partial t} = \overbrace{D_S \Delta S}^{\text{diffusion}} + \overbrace{cPS}^{\text{recruitment gain}} + \overbrace{dP}^{\text{spontaneous misfolding}} - \overbrace{bS}^{\text{degradation}}, \tag{2}$$

with

$$-D_P \nabla P \cdot \hat{n} = -D_S \nabla S \cdot \hat{n} = 0, \text{ on } \partial\Omega_0, \tag{3}$$

$$-D_P \nabla P(x,t) \cdot \hat{n} = \frac{-A}{1 + \left(\frac{\langle S(\cdot,t-t_d)\rangle_i}{S_c}\right)^m}, \text{ on } \partial\Omega_i, \tag{4}$$

$$-D_S \nabla S \cdot \hat{n} = 0, \text{ on } \partial\Omega_i, \tag{5}$$

$$(P(x,0), S(x,0)) = \big(P_0(x), S_0(x)\big), \text{ in } \overline{\Omega}, \tag{6}$$

$$S(x,t) = S_i^*(x,t), \ t \in \big[-t_d, 0\big], \ x \in \partial\Omega_i, \tag{7}$$

for $i = 1,2,3,\ldots,N$. Here $\hat{n}$ denotes the outward normal at the respective boundaries, and

$$\langle S(\cdot, t-t_d)\rangle_i := \frac{1}{|\partial\Omega_i|}\int_{\partial\Omega_i} S(\zeta, t-t_d)\mathrm{d}\zeta,$$

denotes the average PrP$^{\mathrm{Sc}}$ concentration on the cell boundary $\partial\Omega_i$, $i = 1,2,3,\ldots,N$, at time t_d in the past ($t_d \geq 0$). The activation of the UPR is triggered by the high concentration of PrP$^{\mathrm{Sc}}$ near the neuron.

Eqs. (1) and (2) describes the dynamics of PrP$^{\mathrm{C}}$ and PrP$^{\mathrm{Sc}}$, respectively. We assume there is no flux at the brain surface for either protein, which is represented in Eq. (3). Since PrP$^{\mathrm{Sc}}$ is not produced by neurons, there is no flux for PrP$^{\mathrm{Sc}}$ at the cell membrane, which is presented in Eq. (5). Eqs. (6) and (7) represent the initial concentrations of PrP$^{\mathrm{C}}$ and PrP$^{\mathrm{Sc}}$ and the history function of the concentration of PrP$^{\mathrm{Sc}}$. Finally, the UPR mechanism is represented in Eq. (4). The rate at which PrP$^{\mathrm{C}}$ is released at time t decreases as the mean concentration of PrP$^{\mathrm{Sc}}$ at time $t - t_d$ at the cell membrane increases. Mathematically, the magnitude of the flux J_i, of PrP$^{\mathrm{C}}$ from the neuron membrane corresponding neuron i at time t is given by [24]

$$J_i = \frac{A}{1 + \left(\frac{\langle S(\cdot,t-t_d)\rangle_i}{S_c}\right)^m}, \quad i = 1,2,3,\ldots,N.$$

The flux magnitude J_i of PrP$^{\mathrm{C}}$ from neuron i is suppressed as $\langle S(\cdot, t-t_d)\rangle$ increases, with the threshold S_c acting as a switch; the flux is nearer its maximum if $\langle S(\cdot,t-t_d)\rangle_i < S_c$ and closer to zero for $\langle S(\cdot,t-t_d)\rangle_i > S_c$, with larger values of m leading to more step-like behavior. The delay t_d models the fact that during stress, the production of PrP$^{\mathrm{C}}$ cannot shut down immediately; a cascade of signals must be transmitted to decrease PrP$^{\mathrm{C}}$ production, which is represented by the delay t_d. The same principle applies to the increase in PrP$^{\mathrm{C}}$ production when PrP$^{\mathrm{Sc}}$ is cleared. Note that $\hat{n}$ denotes the outward normal at the boundary; hence, for an influx into the extracellular space, the flux appears as negative in Eq. (4).

2.2. Nondimensionalization

Let u_1 and u_2 denote the dimensionless concentrations of the proteins PrP$^{\mathrm{C}}$ and PrP$^{\mathrm{Sc}}$, respectively. To nondimensionalize and rescale Eqs. (1)–(7), we apply the transformations $t = \bar{t}\tilde{t}$, $x = \bar{x}\tilde{x}$, $\Omega = \bar{x}\tilde{\Omega}$, $P(x,t) = \overline{P}u_1(\tilde{x},\tilde{t})$, and $S(x,t) = \overline{S}u_2(\tilde{x},\tilde{t})$, where overbars denote dimensional scales and tildes denote dimensionless variables. Using the substitutions $\bar{t} = \frac{1}{a}$, $\bar{x} = \sqrt{\frac{D_p}{a}}$, $\overline{P} = \frac{A}{\sqrt{D_p a}}$, and $\overline{S} = S_c$, and then simplifying and omitting the tildes, we obtain

$$\begin{cases} \mathbb{L}_j u_j = f_j(u_1,u_2) & \text{in } \Omega_T, \\ \mathbb{B}u_j = 0 & \text{on } \partial\Omega_{0,T}, \\ \mathbb{B}u_1 = \dfrac{1}{1+[\langle u_2(\cdot,t-\tau)\rangle_i]^m} & \text{on } \partial\Omega_{i,T}, \\ \mathbb{B}u_2 = 0 & \text{on } \partial\Omega_{i,T}, \\ u_j(x,0) = u_{0,j}(x) & \text{in } \overline{\Omega}, \\ u_2(x,t) = u_{2,i}^*(x,t) & t \in [-\tau, 0], \ x \in \partial\Omega_i, \end{cases} \tag{8}$$

for $j = 1, 2$ and $i = 1, 2, 3, \dots, N$. Here $\Omega_T = \Omega \times (0, T]$, $\partial\Omega_{i,T} = \partial\Omega_i \times (0, T]$ for some $0 < T < \infty$, and the parabolic operators $\mathbb{L}_j$, boundary operator $\mathbb{B}$, and reaction functions f_j for $j = 1, 2$ are defined as

$$\begin{aligned}
\mathbb{L}_j u &= \frac{\partial u}{\partial t} - \delta_j \Delta u,\\
\mathbb{B}u &= \nabla u \cdot \hat{n},\\
f_1(u_1, u_2) &= -\gamma u_1 u_2 - (1+\sigma)u_1,\\
f_2(u_1, u_2) &= \eta\gamma u_1 u_2 + \eta\sigma u_1 - \beta u_2.
\end{aligned}$$

The definition of nondimensional parameters are listed in Table 1.

Table 1
Dimensionless parameters.

Parameter	Definition	Interpretation
γ	$\frac{cS_c}{a}$	Ratio of (the rate PrP$^{\mathrm{C}}$ is converted to PrP$^{\mathrm{Sc}}$ when S concentration is S_c) to (the rate PrP$^{\mathrm{C}}$ is cleared)
σ	d/a	Ratio of the rate PrP$^{\mathrm{C}}$ spontaneously misfolds to the rate it is cleared
δ_2	D_S/D_P	Ratio of PrP$^{\mathrm{Sc}}$ diffusivity to PrP$^{\mathrm{C}}$ diffusivity
η	$\frac{A}{S_c\sqrt{D_P a}}$	Ratio of characteristic PrP$^{\mathrm{C}}$ concentration to S_c
β	b/a	Ratio of rate PrP$^{\mathrm{Sc}}$ is cleared to the rate PrP$^{\mathrm{C}}$ is cleared
τ	at_d	Delay relative to PrP$^{\mathrm{C}}$ clearance time
$\delta_1 = 1$	Constant value	Chosen for consistency in the model presentation

In this study, we establish the existence of a unique nonnegative strong solution to the system (8) in the space $C(\overline{\Omega}_T) \cap C_x^2(\Omega_T) \cap C_t^1(\Omega_T)$ for every $0 < T < \infty$, and then derive estimates for the concentrations of healthy and toxic proteins. In addition, we present simulations using finite elements. Although the results are demonstrated for $\Omega \subset \mathbb{R}^3$, they are not restricted to three-dimensional domains and can be extended to general $\mathbb{R}^n$. Based on biological observation, we assume the following hypothesis in all our results.

Hypothesis A.

1. $u_{0,j}(x) \geq 0$ and $u_{0,j}(x) \in C\left(\overline{\Omega}\right)$, for $j = 1, 2$;
2. $u^*_{2,i}(x,t) \geq 0$ and $u^*_{2,i}(x,t) \in C\left(\partial\Omega_i \times [-\tau, 0]\right)$, for $i = 1, 2, \dots, N$;
3. $u_2(x, 0) = u^*_{2,i}(x, 0), x \in \partial\Omega_i$, for $i = 1, 2, \dots, N$ (compatibility condition);
4. $m \geq 1$ and $\tau \geq 0$;
5. $\overline{\partial\Omega_i} \cap \overline{\partial\Omega_j} = \emptyset$ for $i, j = 1, 2, \dots, N$ and $i \neq j$;
6. $\partial\Omega$ is a C^2 boundary.

3. Existence and uniqueness

A primary concern in analyzing population models is the global existence of solutions. Additionally, in population dynamics models, it is crucial to ensure that solutions remain nonnegative. Therefore, in this section, we establish the existence of a unique global nonnegative solution to system (8) by constructing suitable upper and lower solutions. We refer the reader to [20] and the references therein for results on different classes of PDEs.

Proposition 1. *Let $f(x,t)$ be Hölder continuous in x for some $\alpha \in (0,1)$, uniformly in $\overline{\Omega}_T$. Then, for any continuous function $h_i(x,t)$ on $\partial\Omega_{i,T}$ for $i = 1, 2, 3, \dots, N$ and any continuous initial data $u_0(x)$ in $\overline{\Omega}$, the boundary value problem*

$$\begin{cases}
\dfrac{\partial u}{\partial t} - \delta\Delta u + Cu = f(x,t) & \text{in } \Omega_T,\\
\nabla u \cdot \hat{n} = h_i(x,t) & \text{on } \partial\Omega_{i,T},\ i = 1, 2, 3, \dots, N,\\
u(x,0) = u_0(x) & \text{in } \overline{\Omega},
\end{cases}$$

where δ is positive constant, C is bounded function, and $\overline{\partial\Omega_i} \cap \overline{\partial\Omega_j} = \emptyset$ for $i \neq j$, admits a unique solution $u \in C_x^2(\Omega_T) \cap C_t^1(\Omega_T)$ that is Hölder continuous in x with Hölder exponent α, uniformly in $\overline{\Omega}_T$. Moreover, $u(x,t) \geq 0$ in $\overline{\Omega}_T$ if f, h_i, and u_0 are nonnegative.

Proof. The proposition is adapted from Theorem 1.2 [20, pp. 52] and Lemma 2.1 [20, pp. 54]. □

Due to the nonlinearity, we use the method of lower and upper solutions to establish the existence of a solution to system (8) with $\tau = 0$. We first prove the existence result for the case $\tau = 0$, and then state the corollary for the case $\tau > 0$.

Since $f_1(u_1, u_2)$ is decreasing in u_2 when $u_1 \geq 0$, and $f_2(u_1, u_2)$ is increasing in u_1 when $u_2 \geq 0$, we adopt the following definition of upper and lower solutions. The definition of upper and lower solutions depends on the monotonicity properties of the reaction terms; see, for instance, [20] and the references therein.

Definition 1. A pair of functions $\hat{\mathbf{u}} = \left(\hat{u}_1, \hat{u}_2\right), \check{\mathbf{u}} = \left(\check{u}_1, \check{u}_2\right)$ in $C(\overline{\Omega}_T) \cap C_x^2\left(\Omega_T\right) \cap C_t^1\left(\Omega_T\right)$ is called an ordered upper and lower solution of (8), respectively, if the functions satisfy the relation $\check{\mathbf{u}} \preccurlyeq \hat{\mathbf{u}}$ and

$$\mathbb{L}_1 \hat{u}_1 - f_1\left(\hat{u}_1, \check{u}_2\right) \geq 0 \geq \mathbb{L}_1 \check{u}_1 - f_1\left(\check{u}_1, \hat{u}_2\right), \tag{9}$$

$$\mathbb{L}_2 \hat{u}_2 - f_2\left(\hat{u}_1, \hat{u}_2\right) \geq 0 \geq \mathbb{L} \check{u}_2 - f_2\left(\check{u}_1, \check{u}_2\right), \tag{10}$$

with

$$\begin{cases} \mathbb{B}\check{u}_j \leq 0 \leq \mathbb{B}\hat{u}_j & \text{on } \partial\Omega_{0,T}, \\ \mathbb{B}\check{u}_2 \leq 0 \leq \mathbb{B}\hat{u}_2 & \text{on } \partial\Omega_{i,T}, \\ \mathbb{B}\check{u}_1 \leq \frac{1}{1+\left(\langle \check{u}_2(\cdot,t)\rangle_i\right)^m} \leq \mathbb{B}\hat{u}_1 & \text{on } \partial\Omega_{i,T}, \\ \check{u}_j(x,0) \leq u_{0,j} \leq \hat{u}_j(x,0) & \text{in } \overline{\Omega}, \end{cases} \tag{11}$$

for $j = 1, 2$ and $i = 1, 2, 3, \dots, N$.

We choose the upper solution $(\hat{u}_1, \hat{u}_2)$ from the solution of the following systems:

$$\begin{cases} \mathbb{L}_1 \hat{u}_1 + (1+\sigma)\hat{u}_1 = K_1 & \text{in } \Omega_T, \\ \mathbb{B}\hat{u}_1 = K_2 & \text{on } \partial\Omega_{i,T}, i = 1, 2, 3, \dots, N, \\ \hat{u}_1(x,0) = M_1 & \text{in } \overline{\Omega}, \end{cases} \tag{12}$$

and

$$\begin{cases} \mathbb{L}_2 \hat{u}_2 + (\beta - \eta\gamma\hat{u}_1)\hat{u}_2 = \eta\sigma\hat{u}_1 + K_3 & \text{in } \Omega_T, \\ \mathbb{B}\hat{u}_2 = K_4 & \text{on } \partial\Omega_{i,T}, i = 1, 2, 3, \dots, N, \\ \hat{u}_2(x,0) = M_2 & \text{in } \overline{\Omega}, \end{cases} \tag{13}$$

where $M_j = \sup\limits_{x \in \overline{\Omega}}\{u_{0,j}(x)\}$ for $j = 1, 2$, $K_2 \geq 1$, $K_4 \geq 0$, $K_1 \geq (1+\sigma)M_1$, and $K_3 \geq \beta M_2$.

Proposition 2. *The systems (12)–(13) admits a unique solution $(\hat{u}_1, \hat{u}_2)$. Moreover, $\hat{u}_1(x,t) \geq M_1$ and $\hat{u}_2(x,t) \geq M_2$ for all $(x,t) \in \overline{\Omega}_T$.*

Proof. By Proposition 1, system (12) admits a unique nonnegative solution $\hat{u}_1$. Substituting $\hat{u}_1$ into (13) and applying the existence theory for linear parabolic equations guarantees the existence of $\hat{u}_2$.
Let $w = \hat{u}_1 - M_1$. Then w satisfies

$$\begin{aligned} \mathbb{L}_1 w + (1+\sigma)w &= \mathbb{L}_1 \hat{u}_1 + (1+\sigma)\hat{u}_1 - (1+\sigma)M_1 \\ &= K_1 - (1+\sigma)M_1, \end{aligned}$$

and since $K_1 \geq (1+\sigma)M_1$, it follows that $\mathbb{L}_1 w + (1+\sigma)w \geq 0$. Together with $\mathbb{B}w \geq 0$ and the initial condition $w(x,0) = 0$, by Proposition 1, we conclude that $w \geq 0$, and therefore $\hat{u}_1 \geq M_1$ in $\overline{\Omega}_T$.

Similarly, let $v = \hat{u}_2 - M_2$. Then v satisfies

$$\begin{aligned} \mathbb{L}_2 v + (\beta - \eta\gamma\hat{u}_1)v &= \mathbb{L}_2 \hat{u}_2 + (\beta - \eta\gamma\hat{u}_1)\hat{u}_2 - (\beta - \eta\gamma\hat{u}_1)M_2 \\ &= \eta\sigma\hat{u}_1 + K_3 - \beta M_2 + \eta\gamma\hat{u}_1 M_2, \end{aligned}$$

and since $K_3 \geq \beta M_2$, it follows that $\mathbb{L}_2 v + (\beta - \eta\gamma\hat{u}_1)v \geq 0$. Together with $\mathbb{B}v \geq 0$ and $v(x,0) = 0$. Again, applying Proposition 1, we deduce that $v \geq 0$, and thus $\hat{u}_2 \geq M_2$ in $\overline{\Omega}_T$. ☐

Lemma 1. *Assume that Hypothesis A holds. Then an ordered pair of upper and lower solutions exists for system (8) with $\tau = 0$.*

Proof. Since $u_{0,j}(x) \geq 0$ for $j = 1, 2$ it is straightforward that the pair $(\check{u}_1, \check{u}_2) = (0, 0)$ and $(\hat{u}_1, \hat{u}_2)$ satisfy the inequalities in (11). We now verify that $(\check{u}_1, \check{u}_2)$ and $(\hat{u}_1, \hat{u}_2)$ satisfy the differential inequalities in (9)–(10):

$$\begin{aligned} &\mathbb{L}_1 \hat{u}_1 - f_1(\hat{u}_1, \check{u}_2) = \mathbb{L}_1 \hat{u}_1 + (1+\sigma)\hat{u}_1 = K_1 \geq 0, \\ &\mathbb{L}_1 \check{u}_1 - f_1(\check{u}_1, \hat{u}_2) = 0, \\ &\mathbb{L}_2 \hat{u}_2 - f_2(\hat{u}_1, \hat{u}_2) = \mathbb{L}_2 \hat{u}_2 + (\beta - \eta\gamma\hat{u}_1)\hat{u}_2 - \eta\sigma\hat{u}_1 = K_3 \geq 0, \\ &\mathbb{L}_2 \check{u}_2 - f_2(\check{u}_1, \check{u}_2) = 0. \end{aligned}$$

Moreover, $(\check{u}_1, \check{u}_2) \preccurlyeq (\hat{u}_1, \hat{u}_2)$ in $\overline{\Omega}_T$. Therefore, $(\hat{u}_1, \hat{u}_2)$ and $(\check{u}_1, \check{u}_2)$ constitute an ordered pair of upper and lower solutions to system (8) with $\tau = 0$. ☐

We construct a solution sector within which the reaction functions satisfy the Lipschitz condition. The solution sector is defined as follows:

$$\mathcal{J} = \{(u_1, u_2) \in C(\overline{\Omega}_T) : (\check{u}_1, \check{u}_2) \preccurlyeq (u_1, u_2) \preccurlyeq (\hat{u}_1, \hat{u}_2)\}.$$

In the sector $\mathcal{J}$, the functions f_j for $j = 1, 2$ satisfy the Lipschitz condition

$$|f_j(u_1, u_2) - f_j(v_1, v_2)| \leq H_j\big(|u_1 - v_1| + |u_2 - v_2|\big), \tag{14}$$

for $(u_1, u_2), (v_1, v_2) \in \mathcal{J}$, and the Hölder continuity condition

$$|f_j(u(x,t), v(x,t)) - f_j(u(y,s), v(y,s))| \leq H_j^*\big(|t-s|^\alpha + |x-y|^\alpha\big), \quad (x,t), (y,s) \in \Omega_T, \tag{15}$$

when $u, v \in C^\alpha(\Omega_T) \cap \mathcal{J}$. Here, H_j and H_j^* denote the Lipschitz and Hölder constants, respectively. Detailed calculations and the explicit forms of these constants are provided in Appendix B.

Let $(\underline{u}_1^{(0)}, \underline{u}_2^{(0)}) = (\check{u}_1, \check{u}_2)$ and $(\overline{u}_1^{(0)}, \overline{u}_2^{(0)}) = (\hat{u}_1, \hat{u}_2)$. For $k = 0, 1, 2, \ldots$ define the sequences $(\underline{u}_1^{(k)}, \underline{u}_2^{(k)})$ and $(\overline{u}_1^{(k)}, \overline{u}_2^{(k)})$ recursively by solving the following system.

$$\begin{cases} \mathbb{L}_1 \overline{u}_1^{(k+1)} + H_1 \overline{u}_1^{(k+1)} = H_1 \overline{u}_1^{(k)} + f_1(\overline{u}_1^{(k)}, \underline{u}_2^{(k)}) \\ \mathbb{L}_1 \underline{u}_1^{(k+1)} + H_1 \underline{u}_1^{(k+1)} = H_1 \underline{u}_1^{(k)} + f_1(\underline{u}_1^{(k)}, \overline{u}_2^{(k)}) \\ \mathbb{L}_2 \overline{u}_2^{(k+1)} + H_2 \overline{u}_2^{(k+1)} = H_2 \overline{u}_2^{(k)} + f_2(\overline{u}_1^{(k)}, \overline{u}_2^{(k)}) \\ \mathbb{L}_2 \underline{u}_2^{(k+1)} + H_2 \underline{u}_2^{(k+1)} = H_2 \underline{u}_2^{(k)} + f_2(\underline{u}_1^{(k)}, \underline{u}_2^{(k)}) \end{cases} \quad \text{in } \Omega_T, \tag{16}$$

with

$$\begin{cases} \mathbb{B} \overline{u}_j^{(k+1)} = 0 = \mathbb{B} \underline{u}_j^{(k+1)} & \text{on } \partial\Omega_{0,T}, \\ \mathbb{B} \overline{u}_2^{(k+1)} = 0 = \mathbb{B} \underline{u}_2^{(k+1)} & \text{on } \partial\Omega_{i,T}, \\ \mathbb{B} \overline{u}_1^{(k+1)} = \frac{1}{1+[\langle \underline{u}_2^{(k)}(\cdot,t)\rangle_i]^m} = \mathbb{B} \underline{u}_1^{(k+1)} & \text{on } \partial\Omega_{i,T}, \\ \overline{u}_j^{(k+1)}(x,0) = u_{0,j}(x) = \underline{u}_j^{(k+1)}(x,0) & \text{in } \overline{\Omega}, \end{cases} \tag{17}$$

for $j = 1, 2$ and $i = 1, 2, 3, \ldots, N$. In the following Lemma we show the well-definedness of sequences $(\underline{u}_1^{(k+1)}, \underline{u}_2^{(k+1)})$ and $(\overline{u}_1^{(k+1)}, \overline{u}_2^{(k+1)})$.

Lemma 2. *For any $(\underline{u}_1^{(0)}, \underline{u}_2^{(0)}), (\overline{u}_1^{(0)}, \overline{u}_2^{(0)}) \in C^\alpha(\Omega_T) \cap C(\overline{\Omega}_T)$, the sequences $(\overline{u}_1^{(k)}, \overline{u}_2^{(k)})$ and $(\underline{u}_1^{(k)}, \underline{u}_2^{(k)})$ generated by the iterations (16) and (17) are well-defined.*

Proof. We establish the existence of $(\overline{u}_1^{(k)}, \overline{u}_2^{(k)})$ and $(\underline{u}_1^{(k)}, \underline{u}_2^{(k)})$ using an induction argument. For $k = 0$, we have

$$\begin{cases} \mathbb{L}_1 \overline{u}_1^{(1)} + H_1 \overline{u}_1^{(1)} = H_1 \overline{u}_1^{(0)} + f_1(\overline{u}_1^{(0)}, \underline{u}_2^{(0)}) \\ \mathbb{L}_1 \underline{u}_1^{(1)} + H_1 \underline{u}_1^{(1)} = H_1 \underline{u}_1^{(0)} + f_1(\underline{u}_1^{(0)}, \overline{u}_2^{(0)}) \\ \mathbb{L}_2 \overline{u}_2^{(1)} + H_2 \overline{u}_2^{(1)} = H_2 \overline{u}_2^{(0)} + f_2(\overline{u}_1^{(0)}, \overline{u}_2^{(0)}) \\ \mathbb{L}_2 \underline{u}_2^{(1)} + H_2 \underline{u}_2^{(1)} = H_2 \underline{u}_2^{(0)} + f_2(\underline{u}_1^{(0)}, \underline{u}_2^{(0)}) \end{cases} \quad \text{in } \Omega_T, \tag{18}$$

with

$$\begin{cases} \mathbb{B} \overline{u}_j^{(1)} = 0 = \mathbb{B} \underline{u}_j^{(1)} & \text{on } \partial\Omega_{0,T}, \\ \mathbb{B} \overline{u}_2^{(1)} = 0 = \mathbb{B} \underline{u}_2^{(1)} & \text{on } \partial\Omega_{i,T}, \\ \mathbb{B} \overline{u}_1^{(1)} = \frac{1}{1+[\langle \underline{u}_2^{(0)}(\cdot,t)\rangle_i]^m} = \mathbb{B} \underline{u}_1^{(1)} & \text{on } \partial\Omega_{i,T}, \\ \overline{u}_j^{(1)}(x,0) = u_{0,j}(x) = \underline{u}_j^{(1)}(x,0) & \text{in } \overline{\Omega}, \end{cases} \tag{19}$$

for $j = 1, 2$ and $i = 1, 2, 3, \ldots, N$. Since $(\underline{u}_1^{(0)}, \underline{u}_2^{(0)}), (\overline{u}_1^{(0)}, \overline{u}_2^{(0)}) \in C^\alpha(\Omega_T)$, the right-hand side functions in system (18) are Hölder continuous and $\frac{1}{1+[\langle \underline{u}_2^{(0)}(\cdot,t)\rangle_i]^m}$ is a continuous function. Hence, by Proposition 1, there exist unique solutions $(\underline{u}_1^{(1)}, \underline{u}_2^{(1)})$ and $(\overline{u}_1^{(1)}, \overline{u}_2^{(1)})$ in $C^\alpha(\Omega_T) \cap C_x^2(\Omega_T) \cap C_t^1(\Omega_T)$. Assume the existence of $(\underline{u}_1^{(k)}, \underline{u}_2^{(k)})$ and $(\overline{u}_1^{(k)}, \overline{u}_2^{(k)})$ in the space $C^\alpha(\Omega_T) \cap C(\overline{\Omega}_T)$. We then prove the existence of the corresponding functions for the next iteration, $k+1$.
Since $(\underline{u}_1^{(k)}, \underline{u}_2^{(k)}), (\overline{u}_1^{(k)}, \overline{u}_2^{(k)}) \in C^\alpha(\Omega_T)$, the functions on the right hand side of (16) belong to $C^\alpha(\Omega_T)$ and $\frac{1}{1+[\langle \underline{u}_2^{(k)}(\cdot,t)\rangle]^m}$ is a continuous function. Hence, there exists a unique solution $(\underline{u}_1^{(k+1)}, \underline{u}_2^{(k+1)})$ and $(\overline{u}_1^{(k+1)}, \overline{u}_2^{(k+1)})$ to systems (16)–(17). □

Lemma 3. *Assume Hypothesis A holds. Let $(\underline{u}_1^{(k)}, \underline{u}_2^{(k)})$ and $(\overline{u}_1^{(k)}, \overline{u}_2^{(k)})$ be the sequences generated by the iterations (16) and (17). Then, for each $k \geq 0$,*

$$\underline{u}_1^{(k)} \leq \underline{u}_1^{(k+1)} \leq \overline{u}_1^{(k+1)} \leq \overline{u}_1^{(k)} \quad \textit{and} \quad \underline{u}_2^{(k)} \leq \underline{u}_2^{(k+1)} \leq \overline{u}_2^{(k+1)} \leq \overline{u}_2^{(k)}.$$

Moreover, the sequences $(\underline{u}_1^{(k)}, \underline{u}_2^{(k)})$ and $(\overline{u}_1^{(k)}, \overline{u}_2^{(k)})$ converge pointwise to the limit functions $(\underline{u}_1, \underline{u}_2)$ and $(\overline{u}_1, \overline{u}_2)$, respectively, and satisfy

$$\check{u}_1 \leq \underline{u}_1 \leq \overline{u}_1 \leq \hat{u}_1,$$
$$\check{u}_2 \leq \underline{u}_2 \leq \overline{u}_2 \leq \hat{u}_2.$$

Proof. Let $w = \overline{u}_1^{(0)} - \overline{u}_1^{(1)}$. Then w satisfies

$$\begin{aligned}
\mathbb{L}_1 w + H_1 w &= (\mathbb{L}_1 \overline{u}_1^{(0)} + H_1 \overline{u}_1^{(0)}) - (\mathbb{L}_1 \overline{u}_1^{(1)} + H_1 \overline{u}_1^{(1)}) \\
&= (\mathbb{L}_1 \overline{u}_1^{(0)} + H_1 \overline{u}_1^{(0)}) - (H_1 \overline{u}_1^{(0)} + f_1(\overline{u}_1^{(0)}, \underline{u}_1^{(0)})) \\
&= \mathbb{L}_1 \hat{u}_1 - f_1(\hat{u}_1, \check{u}_2).
\end{aligned}$$

From Eq. (9), it follows that $\mathbb{L}_1 w + H_1 w \geq 0$. And from (11) and (17) , we have

$$\begin{aligned}
&\mathbb{B}w = \mathbb{B}\overline{u}_1^{(0)} - \mathbb{B}\overline{u}_1^{(1)} = \mathbb{B}\hat{u}_1 \geq 0, \text{ on } \partial\Omega_{0,T}, \\
&\mathbb{B}w = \mathbb{B}\overline{u}_1^{(0)} - \mathbb{B}\overline{u}_1^{(1)} = \mathbb{B}\hat{u}_1 - \frac{1}{1 + [\langle \check{u}_2(\cdot, t)\rangle_i]^m} \geq 0, \text{ on } \partial\Omega_{i,T},\ i = 1, 2, 3, \dots, N.
\end{aligned}$$

By Proposition 1, it follows that $w(x,t) \geq 0$, consequently $\overline{u}_1^{(0)} \geq \overline{u}_1^{(1)}$ in $\overline{\Omega}_T$.

Now, define $w = \underline{u}_1^{(1)} - \underline{u}_1^{(0)}$, then

$$\begin{aligned}
\mathbb{L}_1 w + H_1 w &= (\mathbb{L}_1 \underline{u}_1^{(1)} + H_1 \underline{u}_1^{(1)}) - (\mathbb{L}_1 \underline{u}_1^{(0)} + H_1 \underline{u}_1^{(0)}) \\
&= (H_1 \underline{u}_1^{(0)} + f_1(\underline{u}_1^{(0)}, \overline{u}_2^{(0)})) - (\mathbb{L}_1 \underline{u}_1^{(0)} + H_1 \underline{u}_1^{(0)}) \\
&= f_1(\underline{u}_1^{(0)}, \overline{u}_2^{(0)}) - \mathbb{L}_1 \underline{u}_1^{(0)}.
\end{aligned}$$

From definition of lower and upper solution in Eq. (9), it follows that $\mathbb{L}_1 w + H_1 w \geq 0$. And,

$$\begin{aligned}
&\mathbb{B}w = 0 \quad \text{on } \partial\Omega_{0,T}, \\
&\mathbb{B}w = \mathbb{B}\underline{u}_1^{(1)} - \mathbb{B}\underline{u}_1^{(0)} = \frac{1}{1 + [\langle \check{u}_2(\cdot, t)\rangle_i]^m} - \mathbb{B}\check{u}_1 \geq 0 \quad \text{on } \partial\Omega_{i,T},\ i = 1, 2, 3, \dots, N.
\end{aligned}$$

It implies that, $\underline{u}_1^{(1)} \geq \underline{u}_1^{(0)}$.

Similarly, define $w = \overline{u}_1^{(1)} - \underline{u}_1^{(1)}$, which satisfies

$$\begin{aligned}
\mathbb{L}_1 w + H_1 w &= (\mathbb{L}_1 \overline{u}_1^{(1)} + H_1 \overline{u}_1^{(1)}) - (\mathbb{L}_1 \underline{u}_1^{(1)} + H_1 \underline{u}_1^{(1)}) \\
&= (H_1 \overline{u}_1^{(0)} + f_1(\overline{u}_1^{(0)}, \underline{u}_2^{(0)})) - (H_1 \underline{u}_1^{(0)} + f_1(\underline{u}_1^{(0)}, \overline{u}_2^{(0)})) \\
&= \left[H_1(\overline{u}_1^{(0)} - \underline{u}_1^{(0)}) + f_1(\overline{u}_1^{(0)}, \underline{u}_2^{(0)}) - f_1(\underline{u}_1^{(0)}, \underline{u}_2^{(0)})\right] + \\
&\quad \left[f_1(\underline{u}_1^{(0)}, \underline{u}_2^{(0)}) - f_1(\underline{u}_1^{(0)}, \overline{u}_2^{(0)})\right].
\end{aligned}$$

Since $f_1(u_1, u_2)$ is decreasing in u_2, $f_1(\underline{u}_1^{(0)}, \underline{u}_2^{(0)}) - f_1(\underline{u}_1^{(0)}, \overline{u}_2^{(0)}) \geq 0$ as $\underline{u}_2^{(0)} \leq \overline{u}_2^{(0)}$ and Eq. (14) implies that $\left[H_1(\overline{u}_1^{(0)} - \underline{u}_1^{(0)}) + f_1(\overline{u}_1^{(0)}, \underline{u}_2^{(0)}) - f_1(\underline{u}_1^{(0)}, \underline{u}_2^{(0)})\right] \geq 0$. From the definition of the iteration process in (17), $\mathbb{B}w = 0$ on the boundary. Hence, we conclude that $\overline{u}_1^{(1)} \geq \underline{u}_1^{(1)}$ in $\overline{\Omega}_T$. As a base case, here we proved that $\underline{u}_1^{(0)} \leq \underline{u}_1^{(1)} \leq \overline{u}_1^{(1)} \leq \overline{u}_1^{(0)}$. With similar steps, we conclude that $\underline{u}_2^{(0)} \leq \underline{u}_2^{(1)} \leq \overline{u}_2^{(1)} \leq \overline{u}_2^{(0)}$. From the induction hypothesis, we assume that

$$\underline{u}_1^{(k-1)} \leq \underline{u}_1^{(k)} \leq \overline{u}_1^{(k)} \leq \overline{u}_1^{(k-1)} \quad \text{and} \quad \underline{u}_2^{(k-1)} \leq \underline{u}_2^{(k)} \leq \overline{u}_2^{(k)} \leq \overline{u}_2^{(k-1)},$$

and then we prove the inequality for $k+1$. Let us consider the induction step $w = \overline{u}_1^{(k)} - \overline{u}_1^{(k+1)}$, which satisfies

$$\begin{aligned}
\mathbb{L}_1 w + H_1 w &= \left(\mathbb{L}\overline{u}_1^{(k)} + H_1 \overline{u}_1^{(k)}\right) - \left(\mathbb{L}_1 \overline{u}_1^{(k+1)} + H_1 \overline{u}_1^{(k+1)}\right) \\
&= \left(H_1 \overline{u}_1^{(k-1)} + f_1(\overline{u}_1^{(k-1)}, \underline{u}_2^{(k-1)})\right) - \left(H_1 \overline{u}_1^{(k)} + f_1(\overline{u}_1^{(k)}, \underline{u}_2^{(k)})\right) \\
&= \left[H_1(\overline{u}_1^{(k-1)} - \overline{u}_1^{(k)}) + f_1(\overline{u}_1^{(k-1)}, \underline{u}_2^{(k-1)}) - f_1(\overline{u}_1^{(k)}, \underline{u}_2^{(k-1)})\right] \\
&\qquad + \left[f_1(\overline{u}_1^{(k)}, \underline{u}_2^{(k-1)}) - f_1(\overline{u}_1^{(k)}, \underline{u}_2^{(k)})\right].
\end{aligned}$$

Since $f_1(u_1, u_2)$ is decreasing in u_2, $f_1(\overline{u}_1^{(k)}, \underline{u}_2^{(k-1)}) - f_1(\overline{u}_1^{(k)}, \underline{u}_2^{(k)}) \geq 0$ as $\underline{u}_2^{(k-1)} \leq \overline{u}_2^{(k)}$ and Eq. (14) implies that $\left[H_1(\overline{u}_1^{(k-1)} - \underline{u}_2^{(k)}) + f_1(\overline{u}_1^{(k-1)}, \underline{u}_2^{(k-1)}) - f_1(\overline{u}_1^{(k)}, \underline{u}_2^{(k-1)})\right] \geq 0$. From the definition of iteration process in system (17), $\mathbb{B}w = 0$ on the boundary. Hence, we conclude that $\overline{u}_1^{(k)} \geq \overline{u}_1^{(k+1)}$ in $\overline{\Omega}_T$. With similar steps, we conclude that for $k \geq 0$

$$\underline{u}_1^{(k)} \leq \underline{u}_1^{(k+1)} \leq \overline{u}_1^{(k+1)} \leq \overline{u}_1^{(k)} \quad \text{and} \quad \underline{u}_2^{(k)} \leq \underline{u}_2^{(k+1)} \leq \overline{u}_2^{(k+1)} \leq \overline{u}_2^{(k)}.$$

Since the sequences are monotonic and bounded, it follows that

$$\lim_{k\to\infty} \overline{u}_1^{(k)} = \overline{u}_1,\ \lim_{k\to\infty} \overline{u}_2^{(k)} = \overline{u}_2,\ \lim_{k\to\infty} \underline{u}_1^{(k)} = \underline{u}_1, \text{ and } \lim_{k\to\infty} \underline{u}_2^{(k)} = \underline{u}_2,$$

pointwise. □

Lemma 4. *Let* $(\underline{u}_1, \underline{u}_2)$ *and* $(\overline{u}_1, \overline{u}_2)$ *be the pointwise limits of* $(\overline{u}_1^{(k)}, \overline{u}_2^{(k)})$ *and* $(\underline{u}_1^{(k)}, \underline{u}_2^{(k)})$*, respectively. Then,* $(\underline{u}_1, \underline{u}_2)$ *and* $(\overline{u}_1, \overline{u}_2)$ *are in* $C_x^2(\Omega_T) \cap C_t^1(\Omega_T)$ *and satisfy*

$$\begin{cases} \mathbb{L}_1 \overline{u}_1 = f_1(\overline{u}_1, \underline{u}_2) \\ \mathbb{L}_1 \underline{u}_1 = f_1(\underline{u}_1, \overline{u}_2) \\ \mathbb{L}_2 \overline{u}_2 = f_2(\overline{u}_1, \overline{u}_2) \\ \mathbb{L}_2 \underline{u}_2 = f_2(\underline{u}_1, \underline{u}_2) \end{cases} \quad \text{in } \Omega_T, \tag{20}$$

with

$$\mathbb{B}\overline{u}_j = 0 = \mathbb{B}\underline{u}_j, \text{ on } \partial\Omega_{0,T},$$

$$\mathbb{B}\overline{u}_2 = 0 = \mathbb{B}\underline{u}_2, \text{ on } \partial\Omega_{i,T},$$

$$\mathbb{B}\overline{u}_1 = \frac{1}{1 + [\langle \underline{u}_2(\cdot, t)\rangle_i]^m} = \mathbb{B}\underline{u}_1, \text{ on } \partial\Omega_{i,T},$$

$$\overline{u}_j(x, 0) = u_{0,j}(x) = \underline{u}_j(x, 0), \text{ in } \overline{\Omega},$$

for $j = 1, 2$ and $i = 1, 2, 3, \dots, N$.

Proof. Here, we show that $\mathbb{L}_1 \overline{u}_1 = f_1(\overline{u}_1, \underline{u}_2)$, and the rest of the identities follows by similar arguments. Following the approach in [21, Theorem 2.1], note that from Lemmas 2 and 3, the sequence $\overline{u}_1^{(k)}$ is in $C^\alpha(\Omega_T) \cap C_x^2(\Omega_T) \cap C_t^1(\Omega_T)$ and is uniformly bounded in $C(\overline{\Omega}_T)$, it follows from [21, Theorem 2.1] that there exist positive constants K and δ, independent of k, such that

$$|\overline{u}_1^{(k)}|_{C^\delta(\Omega_T)} \le K, \quad \left| \frac{\partial \overline{u}_1^{(k)}}{\partial x_i} \right|_{C(\Omega_T)} \le K, \quad i = 1, 2, 3. \tag{21}$$

From the definition of the iteration process in (16), we have for $k \ge 0$, $\mathbb{L}_1 \overline{u}_1^{(k+1)} = f_1^{(k+1)}$ in Ω_T, where

$$f_1^{(k+1)} = -H_1 \overline{u}_1^{(k+1)} + H_1 \overline{u}_1^{(k)} + f_1(\overline{u}_1^{(k)}, \underline{u}_2^{(k)}).$$

It is clear that $f_1^{(k+1)}$ is Hölder continuous in Ω_T and uniformly bounded in $C(\overline{\Omega}_T)$. Noting the inequalities in (21) and that $f_1^{(k+1)}$ is Hölder continuous in Ω_T for all k, we obtain a positive constant K^*, independent of k, such that

$$|\overline{f}_1^{(k+1)}|_{C^\delta(\Omega_T)} \le K^*. \tag{22}$$

Also note that, $f_1^{(k+1)}$ converges pointwise to $f_1(\overline{u}_1, \underline{u}_2)$ in Ω_T.

Let Ω'_T be an arbitrary subdomain of Ω_T whose closure lies within Ω_T. Then all the hypotheses of Theorem 15 in [25, p. 80] are satisfied in Ω'_T, as specified in Eqs. (21) and (22). Then there exists a subsequence $\overline{u}_1^{(k')}$ of $\overline{u}_1^{(k)}$ such that

$$\overline{u}_1^{(k')}, \ \frac{\partial \overline{u}_1^{(k')}}{\partial t}, \ \frac{\partial \overline{u}_1^{(k')}}{\partial x_i} \text{ and } \frac{\partial^2 \overline{u}_1^{(k')}}{\partial x_i \partial x_j}, \quad i, j = 1, 2, 3,$$

are uniformly convergent in Ω'_T. This proves that the pointwise limit $\overline{u}_1$ of the sequence $\overline{u}_1^{(k)}$ is in $C_x^2(\Omega_T) \cap C_t^1(\Omega_T)$ and satisfies

$$\mathbb{L}_1 \overline{u}_1 = f_1(\overline{u}_1, \underline{u}_2) \text{ in } \Omega'_T.$$

Since Ω'_T is arbitrary, $\overline{u}_1$ satisfies the above equation in Ω_T. It is clear that $\overline{u}_1$ satisfies the initial condition, i.e.,

$$\lim_{k' \to \infty} \overline{u}_1^{(k')}(x, 0) = u_{0,1} \quad \Longrightarrow \quad \overline{u}_1 = u_{0,1} \quad \text{in} \quad \overline{\Omega}.$$

To show that $\overline{u}_1$ satisfies the boundary condition, we use the same technique as in Theorem 2.1 of [21]. Let (x_0, t_0) be any point on $\partial\Omega_T$. Consider the sequence of functions

$$\xi^{(k)}(r) = \overline{u}_1^{(k)}\big(x_0 + r\hat{n}, \, t_0\big), \quad k = 1, 2, 3, \dots$$

It is clear that $\frac{\mathrm{d}\xi^{(k)}(0)}{\mathrm{d}r} = \frac{\partial \overline{u}_1^{(k)}(x_0, t_0)}{\partial n} = \mathbb{B}\overline{u}_1^{(k)}\Big|_{(x_0, t_0)}$. Since there is a subsequence $\overline{u}_1^{(k'')}$ such that $\frac{\partial \overline{u}_1^{(k'')}}{\partial x_i}$ converges to $\frac{\partial \overline{u}_1}{\partial x_i}$ uniformly in Ω_T as $k'' \to \infty$ for each i, this implies that $\frac{\mathrm{d}\xi^{(k'')}}{\mathrm{d}r}$ converges uniformly. And also, $\xi^{(k'')}(0) = \overline{u}_1^{(k'')}(x_0, t_0)$ converges to $\xi(0) \equiv \overline{u}_1(x_0, t_0)$ as $k'' \to \infty$. Recall that if a sequence $f^{(n)}(\zeta)$ converges at one point in $\zeta_0 \in [a, b]$ as $n \to \infty$, and if the sequence $\frac{\mathrm{d}f^{(n)}}{\mathrm{d}\zeta}$ converges uniformly in $[a, b]$, then $\frac{\mathrm{d}f^{(n)}}{\mathrm{d}\zeta}$ converges to $\frac{\mathrm{d}f}{\mathrm{d}\zeta}$, uniformly in $[a, b]$ [26]. Therefore,

$$\lim_{k'' \to \infty} \frac{\mathrm{d}\xi^{(k'')}(0)}{\mathrm{d}r} = \frac{\mathrm{d}\xi(0)}{\mathrm{d}r},$$

implies that

$$\lim_{k'' \to \infty} \mathbb{B}\overline{u}_1^{(k'')}(x_0, t_0) = \mathbb{B}\overline{u}_1(x_0, t_0).$$

Since $\underline{u}_2^{(k)}$ converges to $\underline{u}_2$ pointwise and is uniformly bounded in Ω_T,

$$\mathbb{B}\bar{u}_1 = \lim_{k''\to\infty} \mathbb{B}\bar{u}_1^{(k'')} = \lim_{k''\to\infty} \frac{1}{1+[\langle \underline{u}_2^{(k'')}(\cdot,t)\rangle]^m} = \frac{1}{1+[\langle \underline{u}_2(\cdot,t)\rangle]^m} \text{ on } \partial\Omega_{i,T},\ i=1,2,3,\dots,N.$$

The remaining identities follow by the same reasoning. □

Remark 1. If $\bar{u}_1 = \underline{u}_1 = u_1$ and $\bar{u}_2 = \underline{u}_2 = u_2$, then (u_1,u_2) is a solution of the system (8) with $\tau = 0$.

Lemma 5. *Let $(\bar{u}_1,\bar{u}_2)$ and $(\underline{u}_1,\underline{u}_2)$ be the pointwise limits of the sequences $(\bar{u}_1^{(k)},\bar{u}_2^{(k)})$ and $(\underline{u}_1^{(k)},\underline{u}_2^{(k)})$, respectively. Then*

$$\bar{u}_1 = \underline{u}_1 \quad \textit{and} \quad \bar{u}_2 = \underline{u}_2 \quad \textit{in } \overline{\Omega}_T.$$

Proof. Define $v_1 = \bar{u}_1 - \underline{u}_1$ and $v_2 = \bar{u}_2 - \underline{u}_2$. From Lemma 4,

$$\begin{cases} \mathbb{L}_j v_j = p_j(v_1,v_2) & \text{in } \Omega_T,\\ \mathbb{B}v_j = 0 & \text{on } \partial\Omega_{i,T},\\ v_j(x,0)=0 & \text{in } \bar{\Omega}, \end{cases} \tag{23}$$

for $j=1,2$ and $i=1,2,3,\dots,N$. Here

$$p_1(v_1,v_2) = -(\gamma\underline{u}_2 + 1 + \sigma)v_1 + \gamma\underline{u}_1 v_2,$$
$$p_2(v_1,v_2) = (\eta\gamma\underline{u}_2 + \eta\sigma)v_1 + (\eta\gamma\underline{u}_1 - \beta)v_2.$$

Since for any fixed $0<T<\infty$, the functions $\underline{u}_1$, $\underline{u}_2$, $\bar{u}_1$, and $\bar{u}_2$ are bounded, there exist constants G_1 and G_2 such that

$$|p_j(w_1,w_2) - p_j(w_1^*,w_2^*)| \le G_j\left(|w_1-w_1^*| + |w_2-w_2^*|\right),\ j=1,2,$$

for (w_1,w_2) and $(w_1^*,w_2^*)\in\mathbb{R}^2$. It is clear that p_1 and p_2 satisfy the Lipschitz condition globally. Hence, by the existence theory for PDEs with global Lipschitz reaction functions (see Theorem 9.1 in [20, pp. 435]), system (23) admits a unique solution $(v_1,v_2)=(0,0)$. Therefore, $u_1 = \bar{u}_1 = \underline{u}_1$ and $u_2 = \bar{u}_2 = \underline{u}_2$. □

Lemma 6. *Assume Hypothesis A holds. Then there exists at most one nonnegative solution (u_1,u_2) to system (8) with $\tau\ge 0$ in $C(\overline{\Omega}_T)\cap C_x^2(\Omega_T)\cap C_t^1(\Omega_T)$ for fixed $0<T<\infty$.*

Proof. Suppose that there exist two solutions (u_1,u_2) and (v_1,v_2). Then $w_1 = u_1 - v_1$ and $w_2 = u_2 - v_2$ satisfy

$$\begin{cases} \mathbb{L}_j w_j = g_j(w_1,w_2) & \text{in } \Omega_T,\\ \mathbb{B}w_j = 0 & \text{on } \partial\Omega_{0,T},\\ \mathbb{B}w_1 = h_i(x,t) & \text{on } \partial\Omega_{i,T},\\ \mathbb{B}w_2 = 0 & \text{on } \partial\Omega_{i,T},\\ w_j(x,0)=0, & \text{in } \bar{\Omega},\\ w_2(x,t) = 0 & t\in[-\tau,0], \end{cases} \tag{24}$$

for $j=1,2$ and $i=1,2,3,\dots,N$. Here

$$g_1(w_1,w_2) = -(\gamma u_2 + 1 + \sigma)w_1 - \gamma v_1 w_2,$$
$$g_2(w_1,w_2) = (\eta\gamma u_2 + \eta\sigma)w_1 + (\eta\gamma v_1 - \beta)w_2,$$

and $h_i(x,t)=0$ if $\tau>0$ on $\partial\Omega_{i,\tau}$ and

$$h_i(x,t) = \frac{1}{1+[\langle u_2(\cdot,t)\rangle_i]^m} - \frac{1}{1+[\langle v_2(\cdot,t)\rangle_i]^m} \quad \text{if } \tau=0 \text{ on } \partial\Omega_{i,T},\ i=1,2,3,\dots,N.$$

The uniqueness for $\tau=0$ is proved first, and the result is subsequently extended to $\tau>0$ using a ladder argument. The energy estimations for w_1 and w_2 are given as

$$\frac{1}{2}\frac{\mathrm{d}}{\mathrm{d}t}\|w_1(\cdot,t)\|^2_{L^2(\Omega)} + \delta_1\|\nabla w_1(\cdot,t)\|^2_{L^2(\Omega)} = \int_\Omega g_1(w_1,w_2)w_1\,\mathrm{d}x + \int_{\partial\Omega} w_1(\hat{n}\cdot\nabla w_1)\,\mathrm{d}\zeta, \tag{25}$$

$$\frac{1}{2}\frac{\mathrm{d}}{\mathrm{d}t}\|w_2(\cdot,t)\|^2_{L^2(\Omega)} + \delta_2\|\nabla w_2(\cdot,t)\|^2_{L^2(\Omega)} = \int_\Omega g_2(w_1,w_2)w_2\,\mathrm{d}x. \tag{26}$$

Adding Eq. (25) and (26), we get

$$\frac{1}{2}\frac{\mathrm{d}}{\mathrm{d}t}\left(\|w_1(\cdot,t)\|^2_{L^2(\Omega)} + \|w_2(\cdot,t)\|^2_{L^2(\Omega)}\right) + \delta_1\|\nabla w_1(\cdot,t)\|^2_{L^2(\Omega)} + \delta_2\|\nabla w_2(\cdot,t)\|^2_{L^2(\Omega)} = I(t) + B(t), \tag{27}$$

where

$$I(t) = \int_\Omega g_1(w_1,w_2)w_1\,\mathrm{d}x + \int_\Omega g_2(w_1,w_2)w_2\,\mathrm{d}x,$$

$$B(t) = \int_{\partial\Omega} w_1(\hat{n}\cdot\nabla w_1)\mathrm{d}\zeta \le \big|[\langle v_2(\cdot,t)\rangle]^m - [\langle u_2(\cdot,t)\rangle]^m\big||\partial\Omega|^{1/2}\|w_1(\cdot,t)\|_{L^2(\partial\Omega)}.$$

For every $\epsilon > 0$, there exist constants $A_1 > 0$, $A_4(\epsilon), A_5(\epsilon), A_6(\epsilon) > 0$ (see Appendix C), such that

$$I(t) \le A_1\Big(\|w_1(\cdot,t)\|^2_{L^2(\Omega)} + \|w_2(\cdot,t)\|^2_{L^2(\Omega)}\Big), \tag{28}$$

$$B(t) \le A_4(\epsilon)\Big(\|w_1(\cdot,t)\|^2_{L^2(\Omega)} + \|w_2(\cdot,t)\|^2_{L^2(\Omega)}\Big) + A_5(\epsilon)\|\nabla w_1(\cdot,t)\|^2_{L^2(\Omega)} + A_6(\epsilon)\|\nabla w_2(\cdot,t)\|^2_{L^2(\Omega)}. \tag{29}$$

Substituting Eqs. (28) and (29) into Eq. (27), and then choosing ϵ such that $\delta_1 > A_5(\epsilon)$, we obtain

$$\frac{1}{2}\frac{\mathrm{d}}{\mathrm{d}t}\Big(\|w_1(\cdot,t)\|^2_{L^2(\Omega)} + \|w_2(\cdot,t)\|^2_{L^2(\Omega)}\Big) \le (A_1 + A_4(\epsilon))\Big(\|w_1(\cdot,t)\|^2_{L^2(\Omega)} + \|w_2(\cdot,t)\|^2_{L^2(\Omega)}\Big).$$

Since $w_1(x,0) = w_2(x,0) = 0$, from the theory of first order linear differential equations we get

$$\|w_1(\cdot,t)\|^2_{L^2(\Omega)} + \|w_2(\cdot,t)\|^2_{L^2(\Omega)} = 0 \text{ for } t \in [0,T].$$

Since w_1 and w_2 are classical solutions, it follows that $w_1(x,t) = 0$ and $w_2(x,t) = 0$. Consequently, $u_1(x,t) = u_2(x,t)$ and $v_1(x,t) = v_2(x,t)$ in $\overline{\Omega}_T$.

Similarly, for $\tau > 0$, we have $B(t) = 0$ in Eq. (27) for $t \in [0,\tau]$. By applying the same argument as above, there exists a unique solution in $[0,\tau]$. Next, consider the problem on $[\tau,2\tau]$ with the initial condition defined at $t = \tau$. Using the same reasoning, there exists at most one solution in $[\tau,2\tau]$. By extending this argument step by step, we obtain uniqueness in $[2\tau,3\tau]$, $[3\tau,4\tau]$, and so on. Hence, system (24) admits a unique solution in $\overline{\Omega}_T$ for $\tau > 0$. □

Theorem 1. *Assume Hypothesis A holds. Then there exists a unique nonnegative solution* $(u_1(x,t),u_2(x,t))$ *to the system* (8) *with* $\tau = 0$ *for* $0 < T < \infty$ *in* $C(\overline{\Omega}_T)\cap C^2_x(\Omega_T)\cap C^1_t(\Omega_T)$.

Proof. The proof of this theorem follows directly from Lemmas 1–6. In Lemma 1, we established the existence of ordered lower and upper solutions, $(0,0)$ and $(\hat{u}_1,\hat{u}_2)$, respectively, in the space $C(\overline{\Omega}_T)\cap C^2_x(\Omega_T)\cap C^1_t(\Omega_T)$. The sequences $(\underline{u}_1^{(k)},\underline{u}_2^{(k)})$ and $(\overline{u}_1^{(k)},\overline{u}_2^{(k)})$, generated by the iterations (16) and (17) with initializations $(\underline{u}_1^{(0)},\underline{u}_2^{(0)}) = (0,0)$ and $(\overline{u}_1^{(0)},\overline{u}_2^{(0)}) = (\hat{u}_1,\hat{u}_2)$, satisfy the monotonicity properties stated in Lemma 3. These sequences converge pointwise to limits $(\underline{u}_1,\underline{u}_2)$ and $(\overline{u}_1,\overline{u}_2)$, respectively.

Finally, the existence of a solution to system (8) is established by showing that $\underline{u}_1 = \overline{u}_1 = u_1$ and $\underline{u}_2 = \overline{u}_2 = u_2$ in Lemma 5. Since $(u_1,u_2)\in\mathcal{J}$, i.e., $(0,0)\le(u_1,u_2)\le(\hat{u}_1,\hat{u}_2)$, this ensures the existence of a nonnegative solution to system (8). The uniqueness of the solution follows from Lemma 6. □

Corollary 1. *Assume Hypothesis A holds. Then there exists a unique nonnegative solution* $(u_1(x,t),u_2(x,t))$ *to the system* (8) *with* $\tau > 0$ *for* $0 < T < \infty$ *in* $C(\overline{\Omega}_T)\cap C^2_x(\Omega_T)\cap C^1_t(\Omega_T)$.

Proof. Since $\tau > 0$, consider the domain $\Omega\times[0,\tau]$, and observe that the problem reduces to

$$\begin{cases} \mathbb{L}_j u_j = f_j(u_1,u_2) & \text{in } \Omega_\tau, \\ \mathbb{B}u_j = 0 & \text{on } \partial\Omega_{0,\tau}, \\ \mathbb{B}u_1 = \dfrac{1}{1+[\langle u^*_{2,i}(\cdot,t-\tau)\rangle_i]^m} & \text{on } \partial\Omega_{i,\tau}, \\ \mathbb{B}u_2 = 0 & \text{on } \partial\Omega_{i,\tau}, \\ u_j(x,0) = u_{0,j}(x) & \text{in } \overline{\Omega}, \end{cases}$$

for $j = 1,2$ and $i = 1,2,3,\dots,N$. Since $u^*_{2,i}(\cdot,t-\tau)$ is a nonnegative and continuous function, the term $\dfrac{1}{1+[\langle u^*_{2,i}(\cdot,t-\tau)\rangle_i]^m}$, $i = 1,2,3,\dots,N$ is a known continuous function. Moreover, as $\dfrac{1}{1+[\langle u^*_{2,i}(\cdot,t-\tau)\rangle_i]^m} \le 1 \le K_2$, for $i = 1,2,3,\dots,N$ in Eq. (12), it follows that $(0,0)$ and $(\hat{u}_1,\hat{u}_2)$ form an ordered pair of lower and upper solutions for system (8) in Ω_τ, respectively. The statements and proofs of Lemmas 1–6 remain valid by setting $T = \tau$ and replacing $\dfrac{1}{1+[\langle u_2(\cdot,t-\tau)\rangle_i]^m}$ by $\dfrac{1}{1+[\langle u^*_{2,i}(\cdot,t-\tau)\rangle_i]^m}$ on $\partial\Omega_{i,\tau}$, for $i = 1,2,3,\dots,N$. Hence, by arguments similar to those in the proof of Theorem 1, we conclude the existence of a unique nonnegative solution to system (8) on $[0,\tau]$.

Next, we shift the problem to the interval $[\tau,2\tau]$, using the solution at $t = \tau$ as the new initial condition. Repetition of the same arguments leads us to conclude the existence of a unique nonnegative solution on $[\tau,2\tau]$. Applying this ladder argument iteratively, we establish the corollary for $[2\tau,3\tau]$ and so on. □

Theorem 1 establishes the existence of a unique nonnegative solution on any finite time interval, implying that the solution does not exhibit finite-time blow-up.

Remark 2. To account for other cells in the brain, we could more generally have defined the region Ω_0 to be the region enclosed by the skull and external to all non-neuronal cells. If we then assumed that there is no flux of PrP$^{\mathrm{C}}$ or PrP$^{\mathrm{Sc}}$ through those other cells, then the boundary conditions on $\partial\Omega$ would be unchanged and our preceding analysis would still hold — the only difference would be that geometrically, $\partial\Omega_0$ would not be connected.

4. Estimations

In this section, we estimate the total concentration of prion proteins at a given time t, and then draw conclusions based on this estimation. The total concentrations of $\mathrm{PrP^C}$ and $\mathrm{PrP^{Sc}}$ at time t are defined as

$$\|u_1(\cdot,t)\|_{L^1(\Omega)} = \int_\Omega |u_1(x,t)|\mathrm{d}x = \int_\Omega u_1(x,t)\mathrm{d}x \quad \text{and} \quad \|u_2(\cdot,t)\|_{L^1(\Omega)} = \int_\Omega |u_2(x,t)|\mathrm{d}x = \int_\Omega u_2(x,t)\mathrm{d}x. \tag{30}$$

Lemma 7. *Assume Hypothesis A holds. Let $(u_1(x,t),u_2(x,t))$ be a nonnegative solution to system (8). Then,*

(i)

$$\|u_1(\cdot,t)\|_{L^1(\Omega)} \le \frac{|\partial\Omega|}{1+\sigma}(1-\exp(-(1+\sigma)t)) + \|u_1(\cdot,0)\|_{L^1(\Omega)}\exp(-(1+\sigma)t), \quad t\ge 0.$$

(ii)

$$\|u_1(\cdot,t)\|^2_{L^2(\Omega)} \le C^2\frac{3|\partial\Omega|}{2(1+\sigma)}(1-\exp(-(1+\sigma)t)) + \|u_1(\cdot,0)\|^2_{L^2(\Omega)}\exp(-(1+\sigma)t),\ t\ge 0,$$

where C is a positive constant independent of x and t. Moreover,

$$\limsup_{t\to\infty}\|u_1(\cdot,t)\|_{L^1(\Omega)} \le \frac{|\partial\Omega|}{1+\sigma} \quad \textit{and} \quad \limsup_{t\to\infty}\|u_1(\cdot,t)\|^2_{L^2(\Omega)} \le C^2\frac{3|\partial\Omega|}{2(1+\sigma)}.$$

(iii)

$$\|u_2(\cdot,t)\|_{L^1(\Omega)} \le \left(\|u_2(x,0)\|_{L^1(\Omega)} + \eta\sigma|\Omega|\int_0^t H(s)\mathrm{d}s\right)\exp\left(\gamma\int_0^t H(s)\mathrm{d}s\right),\ t\ge 0,$$

where $H(t) = \sup_{x\in\overline{\Omega}}\{u_1(x,t)\}$. Moreover, if $\sigma=0$ and $u_2(x,0)=0$, then $u_2(x,t)=0$, in $\overline{\Omega}_T$.

Proof. Proof of statement (i).
Integrating first equation in system (8) for $j=1$ over Ω and then applying divergence theorem, we get

$$\frac{\mathrm{d}}{\mathrm{d}t}\int_\Omega u_1(x,t)\mathrm{d}x = -\gamma\int_\Omega u_1(x,t)u_2(x,t)\mathrm{d}x - (1+\sigma)\int_\Omega u_1(x,t)\mathrm{d}x + \int_{\partial\Omega}\mathbb{B}u_1(\zeta,t)\mathrm{d}\zeta.$$

By noting $(0,0)\preccurlyeq(u_1(x,t),u_2(x,t))$ and $\mathbb{B}u_1(x,t)\le 1$, we have

$$\frac{\mathrm{d}}{\mathrm{d}t}\|u_1(\cdot,t)\|_{L^1(\Omega)} + (1+\sigma)\|u_1(\cdot,t)\|_{L^1(\Omega)} \le |\partial\Omega|. \tag{31}$$

The required estimate follows from Grönwall's inequality, that is

$$\|u_1(\cdot,t)\|_{L^1(\Omega)} \le \frac{|\partial\Omega|}{(1+\sigma)}(1-\exp(-(1+\sigma)t)) + \|u_1(\cdot,0)\|_{L^1(\Omega)}\exp(-(1+\sigma)t), \text{ for } t\ge 0. \tag{32}$$

Proof of statement (ii).
Multiplying u_1 with first equation of system (8) for $j=1$ and then integrating over Ω, we obtain

$$\frac{1}{2}\frac{\mathrm{d}}{\mathrm{d}t}\|u_1(\cdot,t)\|^2_{L^2(\Omega)} + \|\nabla u_1(\cdot,t)\|^2_{L^2(\Omega)} + (1+\sigma)\|u_1(\cdot,t)\|^2_{L^2(\Omega)} = -\gamma\int_\Omega u_2(x,t)|u_1(x,t)|^2\mathrm{d}x + \int_{\partial\Omega}u_1(\zeta,t)\mathbb{B}u_1(\zeta,t)\mathrm{d}\zeta.$$

Noting the nonnegativity of the solution and that $\mathbb{B}u_1\le 1$, and using

$$\int_{\partial\Omega}u_1(\zeta,t)\mathrm{d}\zeta \le |\partial\Omega|^{\frac{1}{2}}\|u_1(\cdot,t)\|_{L^2(\partial\Omega)},$$

we get

$$\frac{1}{2}\frac{\mathrm{d}}{\mathrm{d}t}\|u_1(\cdot,t)\|^2_{L^2(\Omega)} + \|\nabla u_1(\cdot,t)\|^2_{L^2(\Omega)} + (1+\sigma)\|u_1(\cdot,t)\|^2_{L^2(\Omega)} \le |\partial\Omega|^{\frac{1}{2}}\|u_1(\cdot,t)\|_{L^2(\partial\Omega)}.$$

Since for fixed t, $u_1(\cdot,t)\in H_1(\Omega)$, then from the Trace theorem [27], we get

$$\begin{aligned}
|\partial\Omega|^{\frac{1}{2}}\|u_1(\cdot,t)\|_{L^2(\partial\Omega)} &\le |\partial\Omega|^{\frac{1}{2}}C\|u_1(\cdot,t)\|_{H_1(\Omega)}\\
&\le |\partial\Omega|^{\frac{1}{2}}C\left(\|u_1(\cdot,t)\|^2_{L^2(\Omega)} + \|\nabla u_1(\cdot,t)\|^2_{L^2(\Omega)}\right)^{\frac{1}{2}}\\
&\le |\partial\Omega|^{\frac{1}{2}}C\left(\|u_1(\cdot,t)\|_{L^2(\Omega)} + \|\nabla u_1(\cdot,t)\|_{L^2(\Omega)}\right)\\
&= C\left(|\partial\Omega|^{\frac{1}{2}}\|u_1(\cdot,t)\|_{L^2(\Omega)} + |\partial\Omega|^{\frac{1}{2}}\|\nabla u_1(\cdot,t)\|_{L^2(\Omega)}\right)\\
&\le C\left(\frac{|\partial\Omega|}{2\epsilon_1} + \frac{\epsilon_1\|u_1(\cdot,t)\|^2_{L^2(\Omega)}}{2} + \frac{|\partial\Omega|}{2\epsilon_2} + \frac{\epsilon_2\|\nabla u_1(\cdot,t)\|^2_{L^2(\Omega)}}{2}\right),
\end{aligned}$$

for some $\epsilon_1, \epsilon_2 > 0$ and where C is the trace constant that depends on the domain Ω. Then,

$$\frac{1}{2}\frac{\mathrm{d}}{\mathrm{d}t}\|u_1(\cdot,t)\|^2_{L^2(\Omega)} + \left(1 - \frac{C\epsilon_2}{2}\right)\|\nabla u_1(\cdot,t)\|^2_{L^2(\Omega)} + \left(1 + \sigma - \frac{C\epsilon_1}{2}\right)\|u_1(\cdot,t))\|^2_{L^2(\Omega)} \leq \frac{C|\partial\Omega|}{2}\left(\frac{1}{\epsilon_1} + \frac{1}{\epsilon_2}\right).$$

By choosing $\epsilon_2 = \frac{2}{C}$ and $\epsilon_1 = \frac{1+\sigma}{C}$, we get

$$\frac{\mathrm{d}}{\mathrm{d}t}\|u_1(\cdot,t)\|^2_{L^2(\Omega)} + (1+\sigma)\|u_1(\cdot,t)\|^2_{L^2(\Omega)} \leq C^2|\partial\Omega|\left(\frac{1}{1+\sigma} + \frac{1}{2}\right) \leq \frac{3}{2}C^2|\partial\Omega|. \tag{33}$$

Applying Grönwall's inequality to Eq. (33), we get the desired estimation

$$\|u_1(\cdot,t)\|^2_{L^2(\Omega)} \leq C^2\frac{3|\partial\Omega|}{2(1+\sigma)}(1 - \exp(-(1+\sigma)t)) + \|u_1(\cdot,0)\|^2_{L^2(\Omega)}\exp(-(1+\sigma)t), \text{ for } t \geq 0. \tag{34}$$

As $t \to \infty$, Eqs. (32) and (34) yield

$$\limsup_{t\to\infty}\|u_1(\cdot,t)\|_{L^1(\Omega)} \leq \frac{|\partial\Omega|}{1+\sigma}, \quad \text{and} \quad \limsup_{t\to\infty}\|u_1(\cdot,t)\|^2_{L^2(\Omega)} \leq C^2\frac{3|\partial\Omega|}{2(1+\sigma)}. \tag{35}$$

Proof of statement (iii).
Integrating first equation of system (8) for $j = 2$ and applying the divergence theorem, we get

$$\frac{\mathrm{d}}{\mathrm{d}t}\|u_2(\cdot,t)\|_{L^1(\Omega)} \leq \gamma \sup_{x\in\overline{\Omega}}\{u_1(x,t)\}\|u_2(\cdot,t)\|_{L^1(\Omega)} + \eta\sigma\sup_{x\in\overline{\Omega}}\{u_1(x,t)\}|\Omega|.$$

Integrating from 0 to t, we get

$$\|u_2(\cdot,t)\|_{L^1(\Omega)} \leq \|u_2(\cdot,0)\|_{L^1(\Omega)} + \gamma\int_0^t \sup_{x\in\overline{\Omega}}\{u_1(x,s)\}\|u_2(\cdot,s)\|_{L^1(\Omega)}\mathrm{d}s + \eta\sigma|\Omega|\int_0^t \sup_{x\in\overline{\Omega}}\{u_1(x,s)\}\mathrm{d}s.$$

Note that $\|u_2(\cdot,0)\|_{L^1(\Omega)} + \eta\sigma|\Omega|\int_0^t \sup_{x\in\overline{\Omega}}\{u_1(x,s)\}\,\mathrm{d}s$ is a nondecreasing function. Applying Grönwall's inequality implies that

$$\|u_2(\cdot,t)\|_{L^1(\Omega)} \leq \left(\|u_2(\cdot,0)\|_{L^1(\Omega)} + \eta\sigma|\Omega|\int_0^t H(s)\mathrm{d}s\right)\exp\left(\gamma\int_0^t H(s)\mathrm{d}s\right), \text{ for } t \geq 0,$$

where $H(t) = \sup_{x\in\overline{\Omega}}\{u_1(x,t)\}$. If $\sigma = 0$ and $\|u_2(\cdot,0)\|_{L^1(\Omega)} = 0$, we get

$$\|u_2(\cdot,t)\|_{L^1(\Omega)} = 0, \ t \in [0,T].$$

This implies that $u_2(x,t) = 0$. This completes the proof. □

Remark 3. When the L^1 estimate in (35) is re-dimensionalized, we obtain that the lim sup of the total $\mathrm{PrP^C}$ concentration is bounded by a quantity proportional to $\frac{1}{a+d}$. Recall that a and d denote the clearance rate and the spontaneous misfolding rate of $\mathrm{PrP^C}$, respectively. In the limiting case as $a \to \infty$ or $d \to \infty$, the total concentration of $\mathrm{PrP^C}$ tends to zero.

Remark 4. The estimates of $u_2(x,t)$ indicates that the total concentration of $\mathrm{PrP^{Sc}}$ is influenced by the amount of $\mathrm{PrP^C}$ present. This relationship is natural because $\mathrm{PrP^{Sc}}$ proteins primarily accumulate through their interaction with $\mathrm{PrP^C}$, during which $\mathrm{PrP^C}$ is converted into $\mathrm{PrP^{Sc}}$, leading to a gradual increase in $\mathrm{PrP^{Sc}}$ concentration. We estimate $\sup_{0\leq s\leq t}\{H(s)\}$ in Appendix E.

5. Remarks on the asymptotic behavior of proteins

It is important to derive conditions on the dimensionless parameters, such as those related to prion proteins, that ensure the existence of disease-free states. Due to difficulties in finding the steady state solution for system (8), we consider a one-dimensional neuron-centered model, where a single neuron is located at the center of the brain. This assumption introduces planar symmetry in the domain, reducing the spatial domain to the interval $[0,l]$, where $x = 0$ represents the neuron boundary and $x = l$ denotes the brain surface. Under this assumption, the model reduces to

$$\begin{cases} u_{1,t} - u_{1,xx} = -\gamma u_1 u_2 - (1+\sigma)u_1 & x \in [0,l], t > 0, \\ u_{2,t} - \delta_2 u_{2,xx} = \gamma u_1 u_2 + \eta\sigma u_1 - \beta u_2 & x \in [0,l], t > 0, \\ u_{2,x}(0,t) = u_{2,x}(l,t) = 0 & t \geq 0, \\ u_{1,x}(0,t) = \frac{-1}{1+[u_2(0,t-\tau)]^m} \text{ and } u_{1,x}(l,t) = 0 & t \geq 0, \\ u_1(x,0) = u_{0,1} & x \in [0,l], \\ u_2(x,0) = u_{0,2}, \text{ and } u_2(0,t) = u_2^*(0,t) & t \in [-\tau,0], x \in [0,l]. \end{cases} \tag{36}$$

It is clear that if $\eta \neq 0$ and $\sigma \neq 0$, then system (36) does not admit a disease-free state, i.e., $(u_1^s, 0)$, where u_1^s denotes a positive steady-state solution of u_1. Hence, a necessary condition for the existence of a disease-free state is that either $\sigma = 0$ or $\eta = 0$. Here, we derive a sufficient condition such that a disease-free state is locally stable. The time-independent system corresponding to (36) with $\sigma = 0$ is

$$\begin{cases} -u_{1,xx} = -\gamma u_1 u_2 - u_1 \\ -\delta_2 u_{2,xx} = \gamma u_1 u_2 - \beta u_2 \\ u_{2,x}(0) = u_{2,x}(l) = 0 \\ u_{1,x}(0) = \frac{-1}{1+[u_2(0)]^m} \text{ and } u_{1,x}(l) = 0. \end{cases} \tag{37}$$

It is straightforward to see that $(u_1^s, 0)$ is a solution of system (37), where

$$u_1^s = Ae^x + Be^{-x}, \quad A = \frac{e^{-l}}{e^l - e^{-l}} > 0, \quad B = \frac{e^l}{e^l - e^{-l}} > 0. \tag{38}$$

Let $v(x,t)$ and $w(x,t)$ be small perturbations around the equilibrium point. Substituting $u_1(x,t) = u_1^s(x) + v(x,t)$ and $u_2(x,t) = 0 + w(x,t)$ into (36) and linearizing around $(u_1^s, 0)$, we obtain

$$\begin{aligned} v_t - v_{xx} &= -v - \gamma u_1^s w, \\ w_t - \delta_2 w_{xx} &= (\gamma u_1^s - \beta) w, \end{aligned}$$

with

$$\begin{aligned} v_x(0,t) &= c_m w(0, t-\tau), \\ v_x(l,t) &= 0, \\ w_x(0,t) &= w_x(l,t) = 0, \end{aligned}$$

where $c_m = 0$ if $m > 1$ and $c_m = 1$ if $m = 1$.

It is clear from the energy estimation that

$$\frac{\mathrm{d}}{\mathrm{d}t} \|w(\cdot,t)\|^2_{L^2((0,l))} \le 2 \sup_{x\in[0,l]} \{\gamma u_1^s(x) - \beta\} \|w(\cdot,t)\|^2_{L^2((0,l))}.$$

Then

$$\|w(\cdot,t)\|^2_{L^2((0,l))} \le \exp(2G_1 t) \|w(\cdot,0)\|^2_{L^2((0,l))}, \tag{39}$$

where $G_1 := \sup_{x\in[0,l]} \{\gamma u_1^s(x) - \beta\}$. It is straightforward that, if $G_1 < 0$, then

$$\limsup_{t\to\infty} \|w(x,t)\|_{L^2((0,l))} = \limsup_{t\to\infty} \|u_2(x,t)\|_{L^2((0,l))} = 0.$$

And, also if $G_1 < 0$, then there exist some constants $C_1 > 0$ and $G_2 < 0$ such that (see Appendix D)

$$\|w_x(\cdot,t)\|^2_{L^2((0,l))} \le C_1 \exp(G_2 t). \tag{40}$$

The Trace theorem yields the boundary estimate for $w(x,t)$, namely

$$|w(x,t)| \le C\Big(\|w(\cdot,t)\|_{L^2((0,l))} + \|w_x(\cdot,t)\|_{L^2((0,l))} \Big), \quad \text{for } x = 0, l, \tag{41}$$

where $C > 0$ is the trace constant depending on l.
From Eqs. (39) and (40), if $G_1 < 0$, then both $\|w(\cdot,t)\|_{L^2(0,l)}$ and $\|w_x(\cdot,t)\|_{L^2(0,l)}$ decay exponentially. Consequently, Eq. (41) implies that

$$|w(x,t)| \le C_2 \exp(G_3 t), \quad \text{for } x = 0, l, \tag{42}$$

for some constants $C_2 > 0$ and $G_3 < 0$.

Similarly, the energy estimation for $v(x,t)$ is

$$\begin{aligned} \frac{1}{2}\frac{\mathrm{d}}{\mathrm{d}t} \|v(\cdot,t)\|^2_{L^2((0,l))} + \|v_x(\cdot,t)\|^2_{L^2((0,l))} + \|v(\cdot,t)\|^2_{L^2((0,l))} &\le c_m |v(0,t)||w(0,t-\tau)| + \gamma \sup_{x\in(0,l)} \{u_1^s(x)\} \left| \int_0^l vw \mathrm{d}x \right| \\ &\le c_m |v(0,t)||w(0,t-\tau)| \\ &\quad + \gamma \sup_{x\in[0,l]} \{u_1^s(x)\} \left(\frac{\epsilon \|v(\cdot,t)\|^2_{L^2((0,l))}}{2} + \frac{\|w(\cdot,t)\|^2_{L^2((0,l))}}{2\epsilon} \right). \end{aligned} \tag{43}$$

From Young's inequality, we have for any $\epsilon_1 > 0$,

$$c_m |v(0,t)||w(0,t-\tau)| \le c_m \frac{\epsilon_1}{2} |v(0,t)|^2 + c_m \frac{1}{2\epsilon_1} |w(0,t-\tau)|^2. \tag{44}$$

Using the Trace theorem and Eq. (42) in Eq. (44) implies that

$$c_m|v(0,t)|\,|w(0,t-\tau)| \le c_m\frac{\epsilon_1}{2}C_3\left(\|v(\cdot,t)\|^2_{L^2((0,l))}+\|v_x(\cdot,t)\|^2_{L^2((0,l))}\right)+c_m\frac{1}{2\epsilon_1}C_2^2e^{2G_3(t-\tau)}, \tag{45}$$

for some positive constant C_3 depending on l. Substituting Eq. (45) into Eq. (43), we obtain

$$\frac{1}{2}\frac{\mathrm{d}}{\mathrm{d}t}\|v(\cdot,t)\|^2_{L^2((0,l))}+\left(1-c_mC_3\frac{\epsilon_1}{2}-\frac{\gamma\epsilon}{2}\sup_{x\in[0,l]}\{u_1^s(x)\}\right)\|v(\cdot,t)\|^2_{L^2((0,l))}+\left(1-c_mC_3\frac{\epsilon_1}{2}\right)\|v_x(\cdot,t)\|^2_{L^2((0,l))}$$

$$\le c_m\frac{1}{2\epsilon_1}C_2^2e^{2G_3(t-\tau)}+\gamma\sup_{x\in[0,l]}\{u_1^s(x)\}\left(\frac{\|w(\cdot,t)\|^2_{L^2((0,l))}}{2\epsilon}\right).$$

Choosing $\epsilon_1>0$ and $\epsilon>0$ such that

$$G_4:=1-c_mC_3\frac{\epsilon_1}{2}-\frac{\epsilon}{2}\gamma\sup_{x\in[0,l]}\{u_1^s(x)\}>0 \quad\text{and}\quad 1-c_mC_3\frac{\epsilon_1}{2}>0,$$

and using

$$\|w(\cdot,t)\|^2_{L^2((0,l))}\le\|w(\cdot,0)\|^2_{L^2((0,l))}\exp(2G_1t),$$

we obtain

$$\frac{1}{2}\frac{\mathrm{d}}{\mathrm{d}t}\|v(\cdot,t)\|^2_{L^2((0,l))}+G_4\|v(\cdot,t)\|^2_{L^2((0,l))}\le c_m\frac{1}{2\epsilon_1}C_2^2e^{2G_3(t-\tau)}+\gamma\sup_{x\in[0,l]}\{u_1^s(x)\}\frac{\|w(\cdot,0)\|^2_{L^2((0,l))}\exp(2G_1t)}{2\epsilon}.$$

Since $G_4>0$ and if $G_1,G_3<0$, then

$$\limsup_{t\to\infty}\|v(x,t)\|_{L^2((0,l))}=\limsup_{t\to\infty}\|u_1(x,t)-u_1^s(x)\|_{L^2((0,l))}=0.$$

Based on the above calculations, we state sufficient conditions for the asymptotic stability of the disease-free state in the following remark.

Remark 5. If $\sigma=0$, and $G_1=\gamma\sup_{x\in[0,l]}\{Ae^x+Be^{-x}\}-\beta<0$, this condition implies that

$$\gamma(A+B)<\beta,$$

where $A+B=\frac{e^l+e^{-l}}{e^l-e^{-l}}>1$, so the disease-free state is asymptotically stable. Biologically, the dimensionless parameter $\beta=\frac{b}{a}$ denotes the ratio of the rate at which $\mathrm{PrP^{Sc}}$ is cleared to the rate at which $\mathrm{PrP^{C}}$ is cleared, and $\gamma=\dfrac{cS_c}{a}$ denotes the ratio of the rate at which $\mathrm{PrP^{C}}$ is converted into $\mathrm{PrP^{Sc}}$, when the concentration of $\mathrm{PrP^{Sc}}$ is S_c, to the rate at which $\mathrm{PrP^{C}}$ is cleared. The condition $\gamma(A+B)<\beta$ implies that $cS_c(A+B)<b$, which means that when the clearance rate of $\mathrm{PrP^{Sc}}$ is larger than its effective production rate cS_c (the rate of conversion of $\mathrm{PrP^{C}}$ into $\mathrm{PrP^{Sc}}$ when there is no spontaneous misfolding, i.e., $\sigma=0$ and $S=S_c$), the system approaches the disease-free state.

Remark 6. When we consider a one-dimensional problem with two neurons placed at $x=0$ and $x=l$, the model remains the same as system (36) with a small modification in the boundary condition: $u_{1,x}(l,t)=\frac{1}{1+[u_2(l,t-\tau)]^m}$. The conclusion in Remark 5 is still valid, with minor modifications in the constants: $A=\frac{1+e^{-l}}{e^l-e^{-l}}$ and $B=\frac{1+e^l}{e^l-e^{-l}}$. Here l represents the distance between two neurons. As $l\to0$, meaning the neurons are very close to each other, $(A+B)$ becomes very large and the stability condition $\gamma(A+B)<\beta$ becomes more restrictive, requiring a significantly larger clearance rate of $\mathrm{PrP^{Sc}}$ to maintain the disease-free state. In contrast, as $l\to\infty$, meaning the neurons are far apart, the condition approaches $\gamma<\beta$, indicating that the disease-free state is stable whenever the clearance rate of $\mathrm{PrP^{Sc}}$ exceeds its effective production rate.

Here, we derived a sufficient condition for the local asymptotic stability of the disease-free state of the modified model. The UPR may introduce periodic behavior in protein concentration through feedback loops triggered by protein misfolding [18,24]. When misfolded proteins accumulate, the UPR activates signaling mechanisms that slow or temporarily halt the production of healthy proteins, allowing the cell time to restore balance. Once the stress decreases, normal protein synthesis resumes, generating cycles of activation and relaxation that can lead to oscillatory behavior. A more systematic investigation of this phenomenon will be presented in Section 6.1. However, a detailed study of the Hopf bifurcation and the global stability analysis of the original model is left for future investigation.

6. Numerical simulations

Here, we present numerical results illustrating the spatiotemporal distribution of $\mathrm{PrP^{C}}$ and $\mathrm{PrP^{Sc}}$. The governing equations in (8) are solved using the Finite Element Method (FEM). A detailed error and stability analysis of the numerical scheme is beyond the scope of this work and is left for future investigation. To discretize the system in time, we use the Euler scheme with implicit diffusion and explicit reaction. The protein concentration at time step n is given by

$$\frac{u_i^{n+1} - u_i^n}{Dt} = \delta_i \Delta u_i^{n+1} + f_i(u_1^n, u_2^n), \text{ for } i = 1, 2,$$

where $u_i^n \approx u_i(x, t_0 + nDt)$ and Dt is the step size and t_0 is the initial time.
By multiplying with a suitable test function v and integrating over the domain Ω, we get

$$\int_\Omega (u_i^{n+1} - u_i^n) v \mathrm{d}x - Dt \int_\Omega \delta_i \Delta u_i^{n+1} v \mathrm{d}x - Dt \int_\Omega f_i(u_1^n, u_2^n) v \mathrm{d}x = 0, \text{ for } i = 1, 2.$$

By using the divergence theorem, we get

$$\int_\Omega u_2^{n+1} v \mathrm{d}x + Dt \int_\Omega \delta_2 \nabla u_2^{n+1} \cdot \nabla v \mathrm{d}x = \int_\Omega u_2^n v \mathrm{d}x + Dt \int_\Omega f_2(u_1^n, u_2^n) v \mathrm{d}x. \tag{46}$$

and

$$\int_\Omega u_1^{n+1} v \mathrm{d}x + Dt \int_\Omega \delta_1 \nabla u_1^{n+1} \cdot \nabla v \mathrm{d}x - Dt \sum_{i=1}^{N} \int_{\partial\Omega_i} \frac{v}{1 + \frac{1}{|\partial\Omega_i|} \int_{\partial\Omega_i} u_2^{n-k}(y) \mathrm{d}y} \mathrm{d}s = \int_\Omega u_1^n v \mathrm{d}x + Dt \int_\Omega f_1(u_1^n, u_2^n) v \mathrm{d}x, \tag{47}$$

where $u_2^{n-k} \approx u_2(x, t_0 + nDt - kDt)$ and k is the floor value of $\frac{\tau}{Dt}$. The variational form in Eqs. (46)–(47) are used in FEM solver FEniCSx [28] to find the $u_i(x, t)$ for $t > 0$, $i = 1, 2$.

We run numerical simulations in a dimensionless framework where, for simplicity, the brain is modeled as sphere with a diameter of 100 units, while neurons are represented as composite structures, consisting of a spherical soma (head) and a cylindrical axon (tail). In accordance with the literature [29], we consider three neurons, each consisting of a soma with radius 2 units and an axon of length 8 units and thickness 0.5 units, denoted as Neuron 1, Neuron 2, and Neuron 3. The centers of their somas are located at $(0, -6, 0)$, $(6, 6, 0)$, and $(6, -6, 0)$, respectively, within the computational domain, and their axons are directed along the $-\hat{z}$ direction. The domain is discretized using tetrahedral and triangular elements via Gmsh [30], as shown in Fig. 2. Approximately 400,000 elements are used in the simulation (See Appendix F.1), with a time step of $Dt = 0.001$. The surface mesh of the computational domain was generated using Gmsh, as shown in Fig. 2. The initial conditions used in the simulations are described in Appendix F.2.

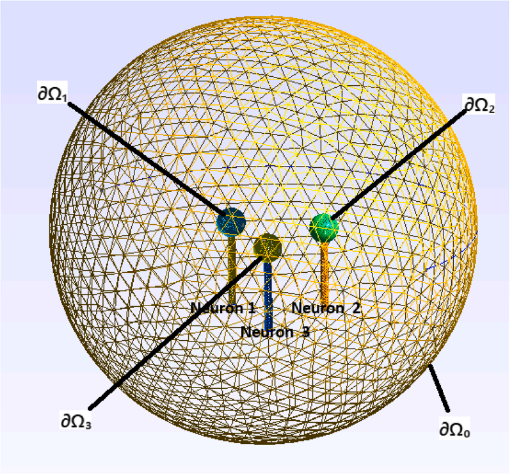

Fig. 2. Discretized computational domain used for the FEM simulations.

Fig. 3 illustrates the spatial spread of protein concentrations in the brain at times $t = 0$, $t = 500$, $t = 1000$, and $t = 1500$, for the parameters $\eta = 1$, $\sigma = 0$, $\delta_2 = 0.1$, $\gamma = 1$, $\beta = 0.3$, and $\tau = 2$. Aside from the sizes, the parameters are quasi-realistic, meaning they approximate biologically relevant values, and are listed in the same order as in [24]. The toxic protein is initially seeded near Neuron 1, and we then observe its progression over time in the absence of spontaneous conversion ($\sigma = 0$). The toxic proteins gradually begin to spread to neighboring neurons due to diffusion. The average concentration of toxic and healthy protein on the cell membrane at time t is calculated from

$$\frac{1}{|\partial\Omega_i|} \int_{\partial\Omega_i} u_2(x, t) \mathrm{d}x \quad \text{and} \quad \frac{1}{|\partial\Omega_i|} \int_{\partial\Omega_i} u_1(x, t) \mathrm{d}x, \quad i = 1, 2, 3 \tag{48}$$

respectively. The average concentration of toxic and healthy proteins on the cell membrane over time is presented in Fig. 4. The short fluctuation observed in the simulation is due to the Gaussian initial profile, which produces a steep concentration gradient and

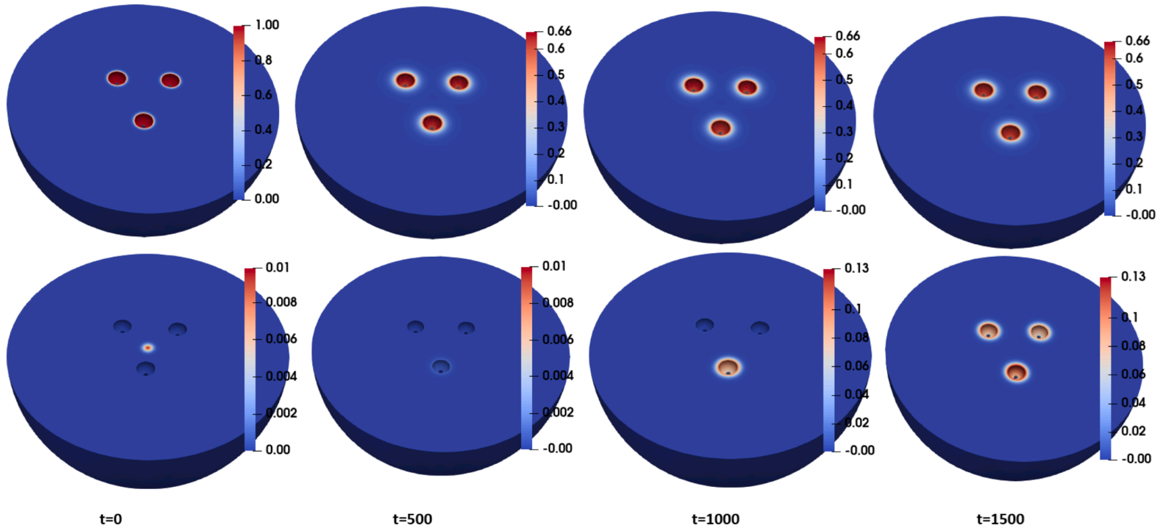

Fig. 3. Spatial distribution of PrP^{C} (top row) and PrP^{Sc} (bottom row) protein concentrations at $t = 0$ (first column), $t = 500$ (second column), $t = 1000$ (third column) , and $t = 1500$ (fouth column), for the parameters $\eta = 1$, $\sigma = 0$, $\delta_2 = 0.1$, $\gamma = 1$, $\beta = 0.3$, and $\tau = 2$.

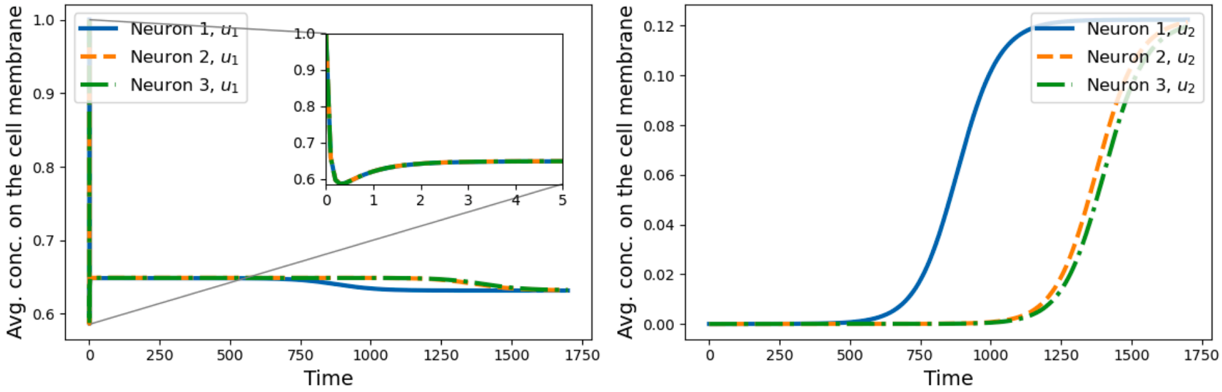

Fig. 4. Average concentration of the PrP^{C} (u_1, left) and PrP^{Sc} (u_2, right) proteins on the cell membranes for the parameters $\eta = 1$, $\sigma = 0$, $\delta_2 = 0.1$, $\gamma = 1$, $\beta = 0.3$, and $\tau = 2$.

results in strong diffusion during the early stage of the simulation. The concentration of toxic protein gradually increases on the cell membrane of Neuron 1, followed by Neuron 2 and Neuron 3, as the initial seeding occurred near Neuron 1.

6.1. Oscillations

Biologically, oscillations in protein concentrations may arise due to the activation of the UPR mechanism. When the concentration of toxic proteins near the cell membrane exceeds a certain threshold, the UPR is triggered. This response suppresses or slows down the production of healthy proteins, allowing the natural clearance or diffusion of toxic proteins. Once the toxic proteins are sufficiently cleared from the vicinity of the cell, neurons resume the production of healthy proteins. This cyclic process may lead to oscillatory behavior in protein concentrations near neuronal membranes.

Mathematically, time delay often induces a Hopf bifurcation at the steady-state solution [18]. However, due to the complexity in determining the steady state of the derived model, we numerically demonstrate the presence of oscillatory behavior for certain parameter regimes.

To investigate the Hopf bifurcation numerically by treating the time delay τ as the bifurcation parameter, we simulate the system for time delays $\tau = 0, 2, 5$, and 7. The corresponding results are presented in Figs. 5–8, respectively. The initial concentrations of toxic and healthy proteins in the brain are discussed in Appendix F.2. Since clearance and diffusion rates are considered critical factors in protein dynamics, we perform numerical experiments by varying $\delta_2 = [0.05, 0.1, 0.2, 0.3]$ and $\beta = [0.1, 0.2, 0.3]$, while keeping $\eta = 1$, $\gamma = 1$, and $\sigma = 0.02$ fixed. Numerical results indicate that the protein dynamics exhibit cyclic behavior as the time delay τ increases for a given set of parameters. Oscillations emerge notably when δ_2 and β are both small, which is consistent with [24].

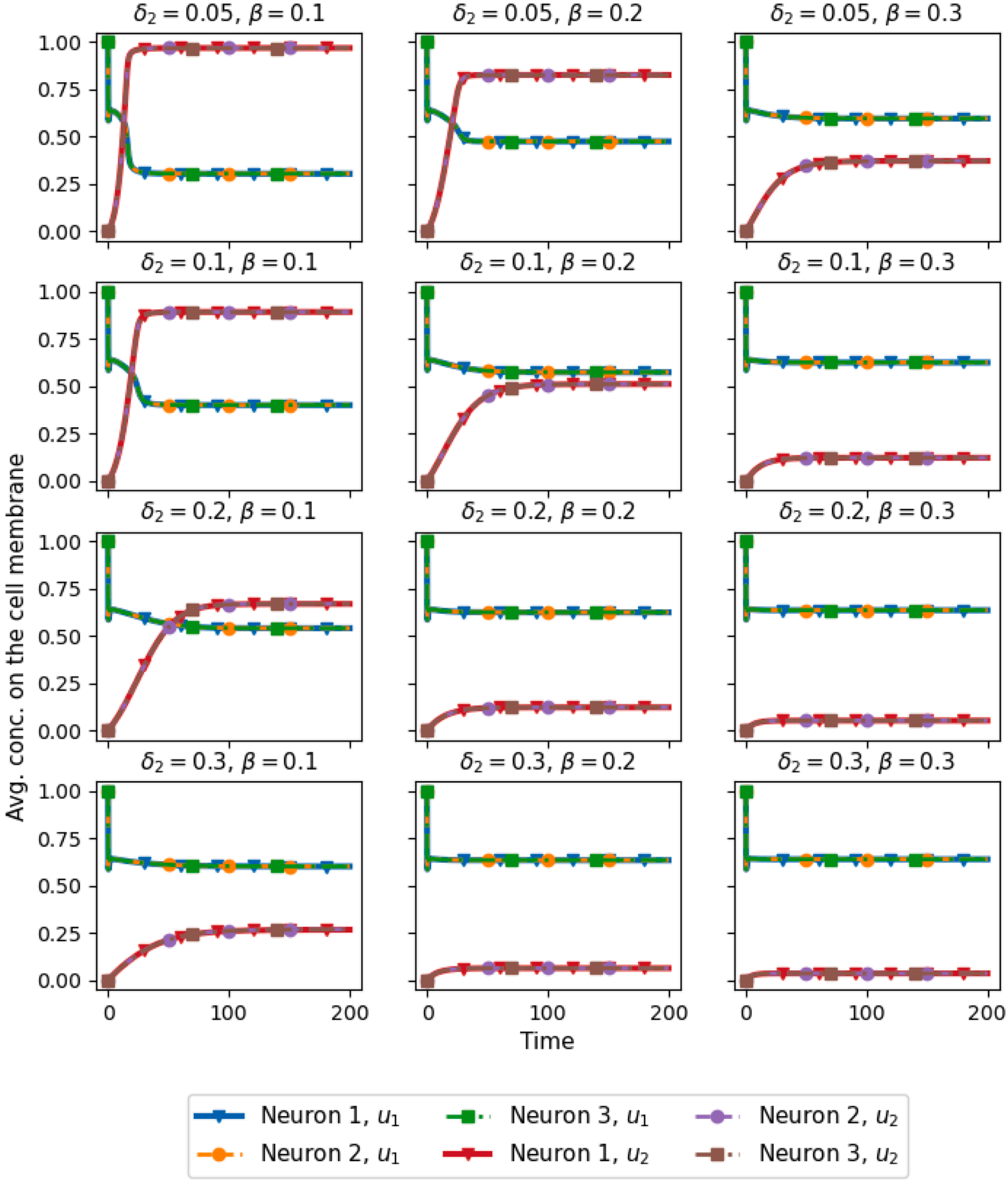

Fig. 5. Average concentration of the PrP^{C} (u_1) and PrP^{Sc} (u_2) proteins on the cell membranes for parameters $\eta = 1$, $\sigma = 0.02$, $\gamma = 1$ and $\tau = 0$.

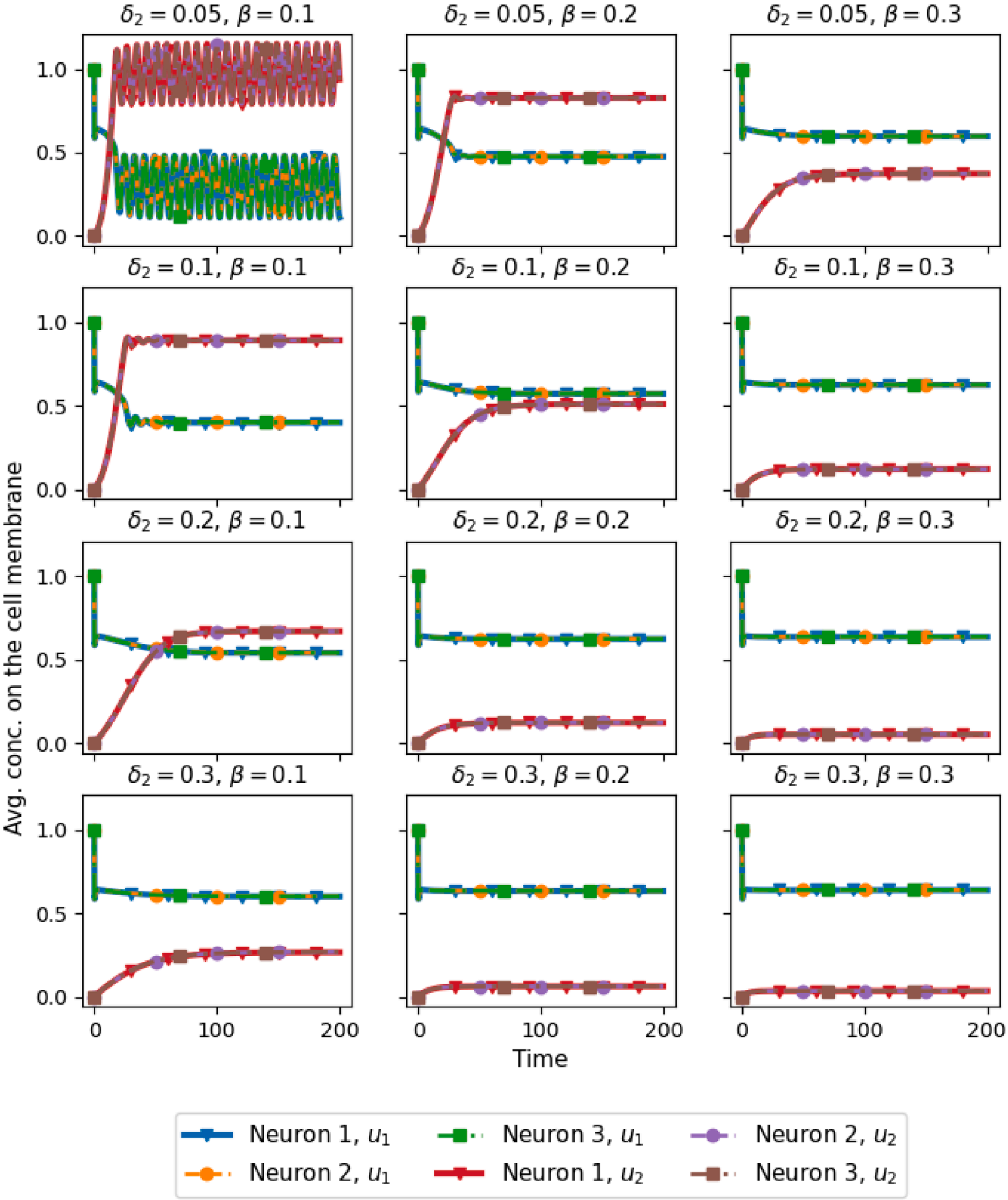

Fig. 6. Average concentration of the PrP^C (u_1) and PrP^{Sc} (u_2) proteins on the cell membranes for parameters $\eta = 1$, $\sigma = 0.02$, $\gamma = 1$ and $\tau = 2$.

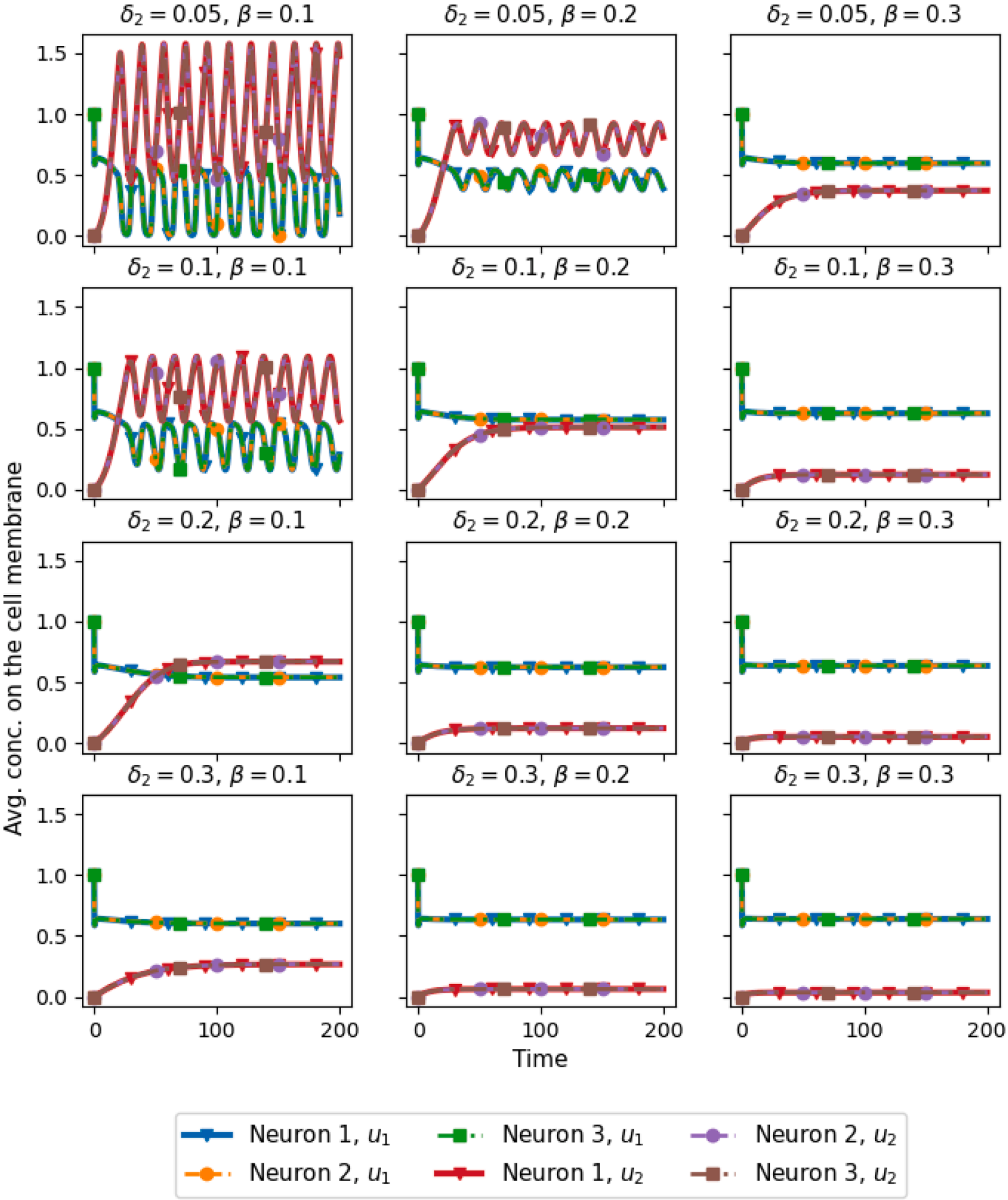

Fig. 7. Average concentration of the $\mathrm{PrP^C}$ (u_1) and $\mathrm{PrP^{Sc}}$ (u_2) proteins on the cell membranes for parameters $\eta = 1$, $\sigma = 0.02$, $\gamma = 1$ and $\tau = 5$.

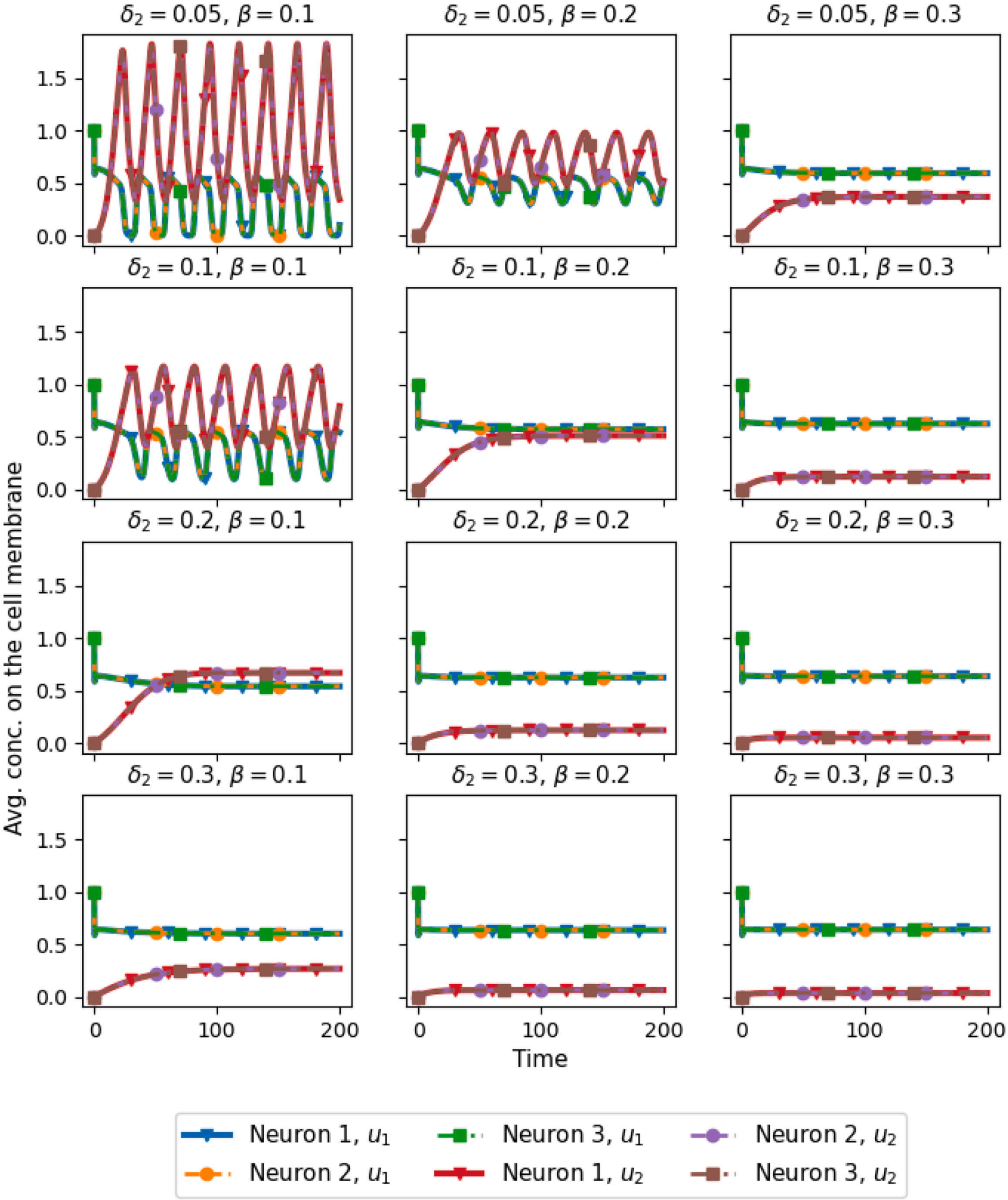

Fig. 8. Average concentration of the PrP^{C} (u_1) and PrP^{Sc} (u_2) proteins on the cell membranes for parameters $\eta = 1$, $\sigma = 0.02$, $\gamma = 1$ and $\tau = 7$.

7. Conclusion and future work

In this work, we analyzed a novel system of nonlinear parabolic partial differential equations with a delayed integral boundary condition to model the progression of prion diseases, incorporating the UPR mechanism. We established the existence and uniqueness of a classical, nonnegative solution to the proposed model. Furthermore, we derived a priori estimates for the total concentration of prion proteins, which enabled us to infer biologically relevant behaviors of disease progression. Numerical simulations were conducted on a simplified three-dimensional geometry using representative parameter values, demonstrating the qualitative dynamics of the system.

In future work, we aim to rigorously identify the parameter regimes under which Hopf bifurcation occurs, thereby providing theoretical insight into the onset of oscillatory behavior observed in the numerical simulations.

Additionally, while this study assumes continuous initial conditions, a natural extension would be to consider initial data with lower regularity and establish existence results in appropriate weak function spaces.

CRediT authorship contribution statement

Gangadhara Boregowda: Writing – review & editing, Writing – original draft, Visualization, Validation, Software, Methodology, Investigation, Formal analysis, Conceptualization; **Laurent Pujo-Menjouet:** Writing – review & editing, Validation, Supervision; **Zhaosheng Feng:** Writing – review & editing, Validation, Supervision; **Michael R. Lindstrom:** Writing – review & editing, Validation, Supervision, Project administration, Investigation, Funding acquisition, Conceptualization.

Data availability

Data will be made available on request.

Declaration of competing interest

The authors declare that they have no competing interests.

Acknowledgments

This work is supported by NSF DMS-2316952.

Appendix A. supporting material

A.1. Notation

Table A.1
List of Notation.

Symbol	Description
$C(\overline{\Omega}_T)$	Space of all continuous functions defined on $\overline{\Omega}_T$.
$C^2_x(\Omega_T) \cap C^1_t(\Omega_T)$	Space of all functions defined on Ω_T that are twice continuously differentiable with respect to the spatial variable x and once continuously differentiable with respect to time t.
$x \preccurlyeq y$	Vector x is element-wise smaller than or equal to vector y
$C^\alpha(\Omega)$	Space of all Hölder continuous functions for some $\alpha \in (0,1)$.
$\lvert u\rvert_{C(\overline{\Omega}_T)}$	$\sup_{(x,t)\in\overline{\Omega}_T} \{u(x,t)\}$
$\lvert\Omega\rvert$	Measure of the domain Ω
H_j	Lipschitz constant of the function f_j.
H^*_j	Hölder constant of the function f_j.
M_j	$\sup_{x\in\overline{\Omega}}\{u_j(x,0)\}$, the supremum of the initial condition u_j over the domain.
$\lVert u\rVert_{H^1(\Omega)}$	H^1 norm of u, defined as $\lVert u\rVert_{H^1(\Omega)} = \left(\lVert u\rVert^2_{L^2(\Omega)} + \lVert\nabla u\rVert^2_{L^2(\Omega)}\right)^{1/2}$.
K_1, K_2, K_3, K_4	Free parameters appearing in the definition of the upper solution, satisfying: $K_1 \geq (1+\sigma)M_1$, $K_2 \geq 1$, $K_3 \geq \beta M_2$, and $K_4 \geq 0$.

A.2. Sobolev embedding theorem

Theorem 2 ([20]). *Let* $n \geq 2$, $\emptyset \neq \Omega \subset \mathbb{R}^n$ *be open with* C^1 *boundary,* $m \in \mathbb{N}$ *and* $1 \leq p < \infty$. *Then,*

$$W^{m,p}(\Omega) \hookrightarrow C^{0,\alpha}(\overline{\Omega}),$$

for $0 < \alpha < m - \frac{n}{p}$ *if* $mp > n > (m-1)p$. *And,*

$$\|u\|_{C^{0,\alpha}(\overline{\Omega})} \leq C_1 \|u\|_{W^{m,p}(\Omega)},$$

where C_1 *depends on* p, m, n *and* Ω.

Appendix B. Properties of reaction function

For $(u_1, u_2), (v_1, v_2) \in \mathcal{J}$,

$$\begin{aligned} |f_1(u_1,u_2) - f_1(v_1,v_2)| &= |-\gamma u_1 u_2 - (1+\sigma)u_1 + \gamma v_1 v_2 + (1+\sigma)v_1| \\ &\leq (1+\sigma+\gamma u_2)|v_1 - u_1| + \gamma v_1 |u_2 - v_2| \\ &\leq H_1(T)(|u_1 - v_1| + |u_2 - v_2|), \end{aligned}$$

where

$$H_1(T) = \max\left\{ \sup_{\overline{\Omega}_T}\{\gamma \hat{u}_1\}, \sup_{\overline{\Omega}_T}\{1+\sigma+\gamma\hat{u}_2\} \right\}.$$

Similarly,

$$\begin{aligned} |f_2(u_1,u_2) - f_2(v_1,v_2)| &= |\eta\gamma u_1 u_2 + \eta\sigma u_1 - \beta u_2 - \eta\gamma v_1 v_2 - \eta\sigma v_1 + \beta v_2| \\ &\leq (\eta\gamma v_2 + \eta\sigma)|u_1 - v_1| + (\eta\gamma u_1 + \beta)|u_2 - v_2| \\ &\leq H_2(T)(|u_1 - v_1| + |u_2 - v_2|), \end{aligned}$$

where

$$H_2(T) = \max\left\{ \sup_{\overline{\Omega}_T}\{\eta\gamma\hat{u}_1 + \beta\}, \sup_{\overline{\Omega}_T}\{\eta\gamma\hat{u}_2 + \eta\sigma\} \right\}.$$

For $u, v \in C^{\alpha}(\overline{\Omega}_T) \cap \mathcal{J}$ and $(x,t), (y,s) \in \overline{\Omega}_T$,

$$\begin{aligned} |f_1(x,t,u(x,t),v(x,t)) - f_1(y,s,u(y,s),v(y,s))| &\leq H_1(|u(x,t) - u(y,s)| + |v(x,t) - v(y,s)|) \\ &\leq H_1^*(|x-y|^{\alpha} + |t-s|^{\alpha}), \end{aligned}$$

where $H_1^*(T) = H_1(T)H_0$, with H_0 being the maximum of the Hölder constants of u and v. Similarly,

$$|f_2(u(x,t),v(x,t)) - f_2(u(y,s),v(y,s))| \leq H_2^*(|x-y|^{\alpha} + |t-s|^{\alpha}).$$

Appendix C. Calculation in Lemma 6

C.1. Bound for $I(t)$

$$I(t) := \int_{\Omega} g_1(w_1,w_2)w_1 \mathrm{d}x + \int_{\Omega} g_2(w_1,w_2)w_2 \mathrm{d}x, \tag{C.1}$$

where

$$\begin{aligned} g_1(w_1,w_2) &= -(\gamma u_2 + 1 + \sigma)w_1 - \gamma v_1 w_2, \\ g_2(w_1,w_2) &= (\eta\gamma u_2 + \eta\sigma)w_1 + (\eta\gamma v_1 - \beta)w_2. \end{aligned}$$

Since (u_1, v_1) and (u_2, v_2) are nonnegative and bounded for $\overline{\Omega}_T$ for any finite $T > 0$, we have

$$g_1(w_1,w_2)w_1 \leq -\gamma v_1 w_1 w_2 \text{ and } g_2(w_1,w_2)w_2 \leq (\eta\gamma u_2 + \eta\sigma)w_1 w_2 + \eta\gamma v_1 w_2^2.$$

Therefore,

$$\int_{\Omega} g_1(w_1,w_2)w_1 \mathrm{d}x \leq |\gamma v_1|_{C(\overline{\Omega}_T)} \left| \int_{\Omega} w_1 w_2 \mathrm{d}x \right| \leq |\gamma v_1|_{C(\overline{\Omega}_T)} \|w_1\|_{L^2(\Omega)} \|w_2\|_{L^2(\Omega)}.$$

Using Young's inequality, we get the following

$$\int_{\Omega} g_1(w_1,w_2)w_1 \mathrm{d}x \leq |\gamma v_1|_{C(\overline{\Omega}_T)} \frac{1}{2}\left(\|w_1\|^2_{L^2(\Omega)} + \|w_2\|^2_{L^2(\Omega)} \right). \tag{C.2}$$

Similarly,

$$\int_\Omega g_2(w_1,w_2)w_2 \mathrm{d}x \le |\eta\gamma u_2+\eta\sigma|_{C(\overline{\Omega}_T)}\frac{1}{2}\Big(\|w_1\|^2_{L^2(\Omega)}+\|w_2\|^2_{L^2(\Omega)}\Big)+|\eta\gamma v_1|_{C(\overline{\Omega}_T)}\|w_2\|^2_{L^2(\Omega)}. \tag{C.3}$$

Substituting Eq. (C.2) and (C.3) in Eq. (C.1), we get

$$I(t) \le A_1\Big(\|w_1\|^2_{L^2(\Omega)}+\|w_2\|^2_{L^2(\Omega)}\Big),$$

where $A_1=\frac{1}{2}|\eta\gamma u_2+\eta\sigma|_{C(\overline{\Omega}_T)}+|\eta\gamma v_1|_{C(\overline{\Omega}_T)}+\frac{1}{2}|\gamma v_1|_{C(\overline{\Omega}_T)}$.

C.2. Bound for B(t)

$$B(t)\le |[\langle v_2(\cdot,t)\rangle]^m-[\langle u_2(\cdot,t)\rangle]^m||\partial\Omega|^{\frac{1}{2}}\|w_1(\cdot,t)\|_{L^2(\partial\Omega)}. \tag{C.4}$$

Since $m\ge 1$, we have for some $A_2>0$

$$|[\langle v_2(\cdot,t)\rangle]^m-[\langle u_2(\cdot,t)\rangle]^m|\le A_2|\langle v_2(\cdot,t)-\langle u_2(\cdot,t)\rangle|=A_2|\langle w_2(\cdot,t)\rangle|\le A_2|\partial\Omega|^{\frac{1}{2}}\|w_2(\cdot,t)\|_{L^2(\partial\Omega)}. \tag{C.5}$$

Substituting Eq. (C.5) in Eq. (C.4) and then using the Trace theorem, we get

$$B(t)\le A_3\big(\|w_1(\cdot,t)\|_{H^1(\Omega)}\big)\big(\|w_2(\cdot,t)\|_{H^1(\Omega)}\big),$$

where $A_3=A_2|\partial\Omega|C^2_{tr}$, C_{tr} is the trace constant, which depends on the domain. From the Rellich–Kondrachov theorem [19], since $H^1(\Omega)$ is compactly embedded in $L^2(\Omega)$ and w_1 and w_2 are bounded in $H^1(\Omega)$, it follows that, for every $\epsilon>0$, there exists a constant $C_\epsilon>0$ such that

$$\|w_1(\cdot,t)\|_{H^1(\Omega)}\le C_\epsilon\|w_1(\cdot,t)\|_{L^2(\Omega)}+\epsilon\|\nabla w_1(\cdot,t)\|_{L^2(\Omega)},$$
$$\|w_2(\cdot,t)\|_{H^1(\Omega)}\le C_\epsilon\|w_2(\cdot,t)\|_{L^2(\Omega)}+\epsilon\|\nabla w_2(\cdot,t)\|_{L^2(\Omega)}.$$

Therefore,

$$B(t)\le A_3\big(C_\epsilon\|w_1(\cdot,t)\|_{L^2(\Omega)}+\epsilon\|\nabla w_1(\cdot,t)\|_{L^2(\Omega)}\|_{H^1(\Omega)}\big)\big(C_\epsilon\|w_2(\cdot,t)\|_{L^2(\Omega)}+\epsilon\|\nabla w_2(\cdot,t)\|_{L^2(\Omega)}\big).$$

After simplifying,

$$\begin{aligned}B(t)\le{}& A_3C_\epsilon^2\|w_1(\cdot,t)\|_{L^2(\Omega)}\|w_2(\cdot,t)\|_{L^2(\Omega)}+A_3C_\epsilon\epsilon\|w_1(\cdot,t)\|_{L^2(\Omega)}\|\nabla w_2(\cdot,t)\|_{L^2(\Omega)}\\&+A_3C_\epsilon\epsilon\|w_2(\cdot,t)\|_{L^2(\Omega)}\|\nabla w_1(\cdot,t)\|_{L^2(\Omega)}+A_3\epsilon^2\|\nabla w_1(\cdot,t)\|_{L^2(\Omega)}\|\nabla w_2(\cdot,t)\|_{L^2(\Omega)}.\end{aligned} \tag{C.6}$$

Using Young's inequality, we get

$$\begin{aligned}A_3C_\epsilon^2\|w_1(\cdot,t)\|_{L^2(\Omega)}\|w_2(\cdot,t)\|_{L^2(\Omega)}&\le\frac{A_3C_\epsilon^2}{2}\Big(\|w_1(\cdot,t)\|^2_{L^2(\Omega)}+\|w_2(\cdot,t)\|^2_{L^2(\Omega)}\Big),\\A_3C_\epsilon\epsilon\|w_1(\cdot,t)\|_{L^2(\Omega)}\|\nabla w_2(\cdot,t)\|_{L^2(\Omega)}&\le\frac{\big(A_3C_\epsilon\epsilon\big)^2}{2\delta_2}\|w_1(\cdot,t)\|^2_{L^2(\Omega)}+\frac{\delta_2}{4}\|\nabla w_2(\cdot,t)\|^2_{L^2(\Omega)},\\A_3C_\epsilon\epsilon\|w_2(\cdot,t)\|_{L^2(\Omega)}\|\nabla w_1(\cdot,t)\|_{L^2(\Omega)}&\le\frac{\big(A_3C_\epsilon\epsilon\big)^2}{2\delta_1}\|w_2(\cdot,t)\|^2_{L^2(\Omega)}+\frac{\delta_1}{4}\|\nabla w_1(\cdot,t)\|^2_{L^2(\Omega)},\\A_3\epsilon^2\|\nabla w_1(\cdot,t)\|_{L^2(\Omega)}\|\nabla w_2(\cdot,t)\|_{L^2(\Omega)}&\le\frac{A_3\epsilon^2}{2}\Big(\|\nabla w_1(\cdot,t)\|^2_{L^2(\Omega)}+\|\nabla w_2(\cdot,t)\|^2_{L^2(\Omega)}\Big).\end{aligned}$$

After substituting above inequalities in Eq. (C.6), we get

$$B(t)\le A_4\big(\|w_1(\cdot,t)\|_{L^2(\Omega)}+\|w_2(\cdot,t)\|_{L^2(\Omega)}\big)+A_5(\epsilon)\|\nabla w_1(\cdot,t)\|_{L^2(\Omega)}+A_6(\epsilon)\|\nabla w_1(\cdot,t)\|_{L^2(\Omega)},$$

where

$$\begin{aligned}A_4(\epsilon)&=\max\left\{\frac{A_3C_\epsilon^2}{2}+\frac{\big(A_3C_\epsilon\epsilon\big)^2}{2\delta_2},\frac{A_3C_\epsilon^2}{2}+\frac{\big(A_3C_\epsilon\epsilon\big)^2}{2\delta_1}\right\},\\A_5(\epsilon)&=\frac{\delta_1}{4}+\frac{A_3\epsilon^2}{2},\\A_6(\epsilon)&=\frac{\delta_2}{4}+\frac{A_3\epsilon^2}{2}.\end{aligned}$$

Appendix D. Estimation of $w_x(x,t)$

Consider

$$w_t - \delta_2 w_{xx} = (\gamma u_1^s - \beta)w, \tag{D.1}$$

with $w_x(0) = w_x(l) = 0$ and $G_1 = \sup_{x\in[0,l]}\{\gamma u_1^s(x) - \beta\} < 0$. Where u_1^s mentioned in (38). Differentiating Eq. (D.1) with respect to x and denoting $z = w_x$, we get

$$z_t - \delta_2 z_{xx} = (\gamma u_1^s - \beta)z + \gamma u_{1,x}^s w, \tag{D.2}$$

with $z(0) = z(l) = 0$.

The energy estimation for z gives the following

$$\begin{aligned}
\frac{1}{2}\frac{\mathrm{d}}{\mathrm{d}t}\|z(\cdot,t)\|^2_{L^2((0,l))} &\le G_1\|z(\cdot,t)\|^2_{L^2((0,l))} + \sup_{x\in[0,l]}|\gamma u_{1,x}^s|\left|\int_0^l w(x,t)z(x,t)\mathrm{d}x\right| \\
&\le G_1\|z(\cdot,t)\|^2_{L^2((0,l))} + \sup_{x\in[0,l]}|\gamma u_{1,x}^s|\left(\|w(\cdot,t)\|_{L^2((0,l))}\|z(\cdot,t)\|_{L^2((0,l))}\right) \\
&\le G_1\|z(\cdot,t)\|^2_{L^2((0,l))} + \sup_{x\in[0,l]}|\gamma u_{1,x}^s|\left(\frac{\|w(\cdot,t)\|^2_{L^2((0,l))}}{2\epsilon} + \frac{\epsilon\|z(\cdot,t)\|^2_{L^2((0,l))}}{2}\right) \\
&\le \left(G_1 + \frac{\epsilon}{2}\sup_{x\in[0,l]}|\gamma u_{1,x}^s|\right)\|z(\cdot,t)\|^2_{L^2((0,l))} + \sup_{x\in[0,l]}|\gamma u_{1,x}^s|\frac{\|w(\cdot,t)\|^2_{L^2((0,l))}}{2\epsilon}.
\end{aligned}$$

We choose ϵ such that

$$G_5 = G_1 + \tfrac{\epsilon}{2}\sup_{x\in[0,l]}\left|\gamma u_{1,x}^s\right| < 0.$$

Then, from Eq. (39),

$$\|w(\cdot,t)\|^2_{L^2((0,l))} \le \exp(2G_1 t)\,\|w(\cdot,0)\|^2_{L^2((0,l))},$$

we get

$$\frac{1}{2}\frac{\mathrm{d}}{\mathrm{d}t}\|z(\cdot,t)\|^2_{L^2((0,l))} \le G_5\|z(\cdot,t)\|^2_{L^2((0,l))} + C_4\exp(2G_1 t), \tag{D.3}$$

where $C_4 = \frac{1}{2\epsilon}\sup_{x\in[0,l]}|\gamma u_{1,x}^s|\|w(\cdot,0)\|^2_{L^2((0,l))}$. Solving the above linear differential inequalities, we obtain an exponential decay of $\|z(\cdot,t)\|^2_{L^2((0,l))} = \|w_x(\cdot,t)\|^2_{L^2((0,l))}$, i.e., there exist some constants, $C_1 > 0$ and $G_2 < 0$ such that

$$\|w_x(\cdot,t)\|^2_{L^2((0,l))} \le C_1\exp(G_2 t), \tag{D.4}$$

where $G_2 = 2G_5$ and $C_1 = \left(\frac{2C_4}{\epsilon\sup_{x\in[0,l]}|\gamma u_{1,x}^s|}\left(1 - \exp(-\epsilon\sup_{x\in[0,l]}|\gamma u_{1,x}^s|)\right) + \|w_x(x,0)\|^2_{L^2((0,l))}\right)$.

Appendix E. Estimation of $H(t) = \sup_{x\in\overline{\Omega}}\{|u_1(x,t)|\}$

Noting that $0 \le u_1(x,t) \le \hat{u}_1(x,t)$, the estimate of $H(t)$ follows directly from the estimate of $\sup_{x\in\overline{\Omega}}\{|\hat{u}_1(x,t)|\}$. Let $v(x,t) = A(t) + \phi(x)$, where

$$A'(t) + (1+\sigma)A(t) = 0, \quad A(0) = M_1, \tag{E.1}$$

and

$$-\Delta\phi + (1+\sigma)\phi = K_1 \text{ in } \Omega \quad \text{and } \mathbb{B}\phi = K_2 \text{ on } \partial\Omega_i \text{ for } i = 0,1,2,3,\ldots,N, \tag{E.2}$$

where M_1, K_1, and K_2 are defined in Eq. (12). Since K_1 and K_2 are nonnegative, it follows that $\phi(x) \ge 0$. Consequently, $v(x,t)$ satisfies

$$\begin{cases}
v_t - \Delta v + (1+\sigma)v = K_1, & \text{in } \Omega_T, \\
\mathbb{B}v = K_2, & \text{on } \partial\Omega_{i,T}, \text{ i=1,2,3,...,N}, \\
v(x,0) = M_1 + \phi(x). & \text{in } \overline{\Omega},
\end{cases} \tag{E.3}$$

Since $v(x,0) \ge \hat{u}_1(x,0)$, and by applying the comparison theorem for parabolic differential equations (see Theorem 2.1 in [20, pp. 55]) to Eqs. (12) and (E.3), we have

$$\hat{u}_1(x,t) \le v(x,t) \text{ in } \overline{\Omega}_T. \tag{E.4}$$

Eqs. (E.1)–(E.2), yield

$$v(x,t) = M_1 \exp\left(-(1+\sigma)t\right) + \phi(x).$$

Then,

$$\sup_{x\in\overline{\Omega}}\{|\hat{u}_1(x,t)|\} \le M_1 \exp\left(-(1+\sigma)t\right) + \sup_{x\in\Omega}\{|\phi(x)|\}. \tag{E.5}$$

From the estimation of elliptic PDEs (see Lemma 1.1 [20, pp. 95]), we have for some K that

$$\|\phi\|_{H^2(\Omega)} \le K\left(\|K_1\|_{L^2(\Omega)} + \|K_2\|_{1,1/2}\right),$$

where

$$\|K_2\|_{m,1/p} \equiv \inf\{\|u\|_{W^{m,p}(\Omega)} \mid u \in C^m(\overline{\Omega}) \text{ and } u = K_2 \quad \text{on } \partial\Omega\}.$$

Since $\Omega \subset \mathbb{R}^3$, $H^2(\Omega) \hookrightarrow C^{0,1/2}(\overline{\Omega})$ (see Sobolev Embedding Theorem 2). Then

$$\sup_{x\in\overline{\Omega}}\{|\phi(x)|\} \le C_1\|\phi\|_{H^2(\Omega)} \le C_2 K\left(\|K_1\|_{L^2(\Omega)} + \|K_2\|_{1,1/2}\right). \tag{E.6}$$

where C_2 is a constant that depends on Ω. Using $K_1 = (1+\sigma)M_1$ and Eq. (E.6) in Eq. (E.5), we get

$$H(t) = \sup_{x\in\overline{\Omega}}\{|\hat{u}_1(x,t)|\} \le M_1 \exp\left(-(1+\sigma)t\right) + C_2 K\left((1+\sigma)M_1|\Omega|^{\frac{1}{2}} + \|K_2\|_{1,1/2}\right).$$

Taking the supremum over $[0,t]$, we get

$$\sup_{0\le s\le t}\{H(s)\} \le M_1 + C_2 K\left((1+\sigma)M_1|\Omega|^{\frac{1}{2}} + \|K_2\|_{1,1/2}\right).$$

Appendix F. Numerical Simulation Framework

F.1. Mesh analysis

To minimize the impact of discretization on the FEM solution, we compute the total concentration of the healthy and toxic proteins, namely

$$\int_\Omega u_1(x,t)\,\mathrm{d}x \quad \text{and} \quad \int_\Omega u_2(x,t)\,\mathrm{d}x,$$

for varying mesh resolutions (i.e., different element sizes or total number of elements, N_e). Based on our simulations, we observe numerically that the FEM solution attains convergence with approximately 4×10^5 elements. Consequently, a mesh of this size is employed in all the simulations presented in the numerical section. (See Fig. F.1).

F.2. Initial condition

The toxic protein $u_2(x,0)$ was initially seeded in the center of the brain, i.e., $(0,0,0)$ and using the Gaussian function

$$u_2(x,0) = 0.01\exp\left(-|x|^2\right), \quad x \in \overline{\Omega}.$$

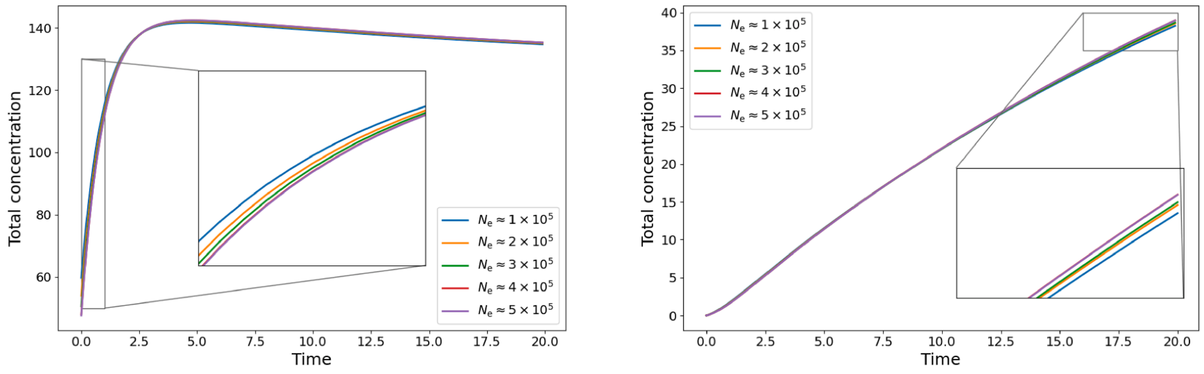

(a)

(b)

Fig. F.1. Mesh convergence study: (A) Total concentration of PrP$^{\mathrm{C}}$ (u_1) in the brain. (B) Total concentration of PrP$^{\mathrm{Sc}}$ (u_2) in the brain.

Note that $u_2(x,0) \approx 0$ at cell membrane and brain surface. See plots ($t = 0$) in Fig. 3. To satisfy the compatibility condition with history function, we require

$$u_2(x,0) = u^*_{2,i}(x,0), \quad x \in \partial\Omega_i,\ i = 1,2,3.$$

Therefore, for simplicity, we assume

$$u^*_{2,i}(x,t) = 0, \quad x \in \partial\Omega_i,\ t \in [-\tau,0],\ i = 1,2,3. \tag{F.1}$$

Substituting Eq. (F.1) into the flux boundary condition, we get

$$\nabla u_1(x,0) \cdot \hat{n} = 1, \quad \text{on } \partial\Omega_i,\ i = 1,2,3.$$

Since the cellular prion protein, $\mathrm{PrP^C}$, is produced within neurons and resides in close proximity to the neuron, we choose the initial concentration of $\mathrm{PrP^C}$ as a sum of Gaussian functions, defined as follows

$$u_1(x,0) = \sum_{i=1}^{3} a_i \exp\left(-b_i\left(|x - x_i|^2 - r^2\right)\right), \quad x \in \overline{\Omega},$$

where $x_i \in \mathbb{R}^3$ denotes the center of neuron i, $r = 2$ is the neuronal radius, and a_i, b_i are parameters chosen such that $\nabla u_1(x,0) \cdot \hat{n} \approx 1$. For simplicity, we set $a_i = b_i = 1$ for $i = 1,2,3$. Note that $u_1(x,0)$ does not exactly satisfy the boundary condition at $t = 0$, but $\nabla u_1(x,0) \cdot \hat{n} \approx 1$.

References

[1] Adimy M, Babin L, Pujo-Menjouet L. Neuron scale modeling of prion production with the unfolded protein response. SIAM J Appl Dyn Syst 2022;21(4):2487–517.
[2] Saqlain M, Alam M, Rönnegård L, Westin J. Investigating stochastic differential equations modelling for levodopa infusion in patients with parkinson's disease. Eur J Drug Metab Pharmacokinet 2020;45:41–9.
[3] Raj A, Kuceyeski A, Weiner M. A network diffusion model of disease progression in dementia. Neuron 2012;73(6):1204–15.
[4] Assembly F. An analytical solution to the kinetics of breakable. Geology 2002;30:251.
[5] Weickenmeier J, Jucker M, Goriely A, Kuhl E. A physics-based model explains the prion-like features of neurodegeneration in Alzheimer's disease, Parkinson's disease, and amyotrophic lateral sclerosis. J Mech Phys Solids 2019;124:264–81.
[6] Atkinson CJ, Zhang K, Munn AL, Wiegmans A, Wei MQ. Prion protein scrapie and the normal cellular prion protein. Prion 2016;10(1):63–82.
[7] Selkoe DJ. Folding proteins in fatal ways. Nature 2003;426(6968):900–4.
[8] Moreno JA, Radford H, Peretti D, Steinert JR, Verity N, Martin MG, et al. Sustained translational repression by eIF2α-p mediates prion neurodegeneration. Nature 2012;485(7399):507–11.
[9] Kiaei M. New hopes and challenges for treatment of neurodegenerative disorders: great opportunities for young neuroscientists. Basic Clin Neurosci 2013;4(1):3.
[10] Knabner P, Angermann L. Numerical methods for elliptic and parabolic partial differential equations. Springer; 2003.
[11] Zienkiewicz OC, Taylor RL. The finite element method for solid and structural mechanics. Elsevier; 2005.
[12] Guo S. Bifurcation in a reaction-diffusion model with nonlocal delay effect and nonlinear boundary condition. J Differ Equ 2021;289:236–78.
[13] Guo S. Global dynamics of a Lotka-Volterra competition-diffusion system with nonlinear boundary conditions. J Differ Equ 2023;352:308–53.
[14] Arrieta JM, Carvalho AN, Rodriguez-Bernal A. Parabolic problems with nonlinear boundary conditions and critical nonlinearities. J Differ Eqs 1999;156(2):376–406.
[15] Pao CV. Time delayed parabolic systems with coupled nonlinear boundary conditions. Proc Am Math Soc 2002;130(4):1079–86.
[16] Magal P, Ruan S. Theory and applications of abstract semilinear Cauchy problems. Springer; 2018.
[17] Travis CC, Webb GF. Existence and stability for partial functional differential equations. Trans Am Math Soc 1974;200:395–418.
[18] Boregowda G, Lindstrom MR. Existence and stability theory of a neurologically inspired parabolic PDE model with a nonlinear time-delayed boundary condition. Int J Bifurcation Chaos 2025;2550170.
[19] Brezis H. Functional Analysis, Sobolev Spaces and Partial Differential Equations. Springer Science & Business Media; 2011.
[20] Pao CV. Nonlinear parabolic and elliptic equations. Springer Science & Business Media; 2012.
[21] Pao CV, Ruan WH. Positive solutions of quasilinear parabolic systems with nonlinear boundary conditions. J Math Anal Appl 2007;333(1):472–99.
[22] Shafiq M, Da Vela S, Amin L, Younas N, Harris DA, Zerr I, et al. The prion protein and its ligands: insights into structure-function relationships. Biocht Biophys Acta (BBA)-Mol Cell Res 2022;1869(6):119240.
[23] Smith HL, Mallucci GR. The unfolded protein response: mechanisms and therapy of neurodegeneration. Brain 2016;139(8):2113–21.
[24] Miller EM, Chan T CD, Montes-Matamoros C, Sharif O, Pujo-Menjouet L, Lindstrom MR. Oscillations in neuronal activity: a neuron-centered spatiotemporal model of the unfolded protein response in prion diseases. Bull Math Biol 2024;86(7):82.
[25] Friedman A. Partial differential equations of parabolic type. Courier Dover Publications; 2008.
[26] Rudin W. Principles of Mathematical Analysis. New York: McGraw-Hill; 3 rd.; 1976.
[27] Evans LC. Partial differential equations. American Mathematical Society; 2022.
[28] Alnæs MS, Logg A, Ølgaard KB, Rognes ME, Wells GN. Unified form language: a domain-specific language for weak formulations of partial differential equations. ACM Trans Math Softw (TOMS) 2014;40(2):1–37.
[29] Andrade-Restrepo M, Lemarre P, Pujo-Menjouet L, Tine LM, Ciuperca SI. Modeling the spatial propagation of Aβ oligomers in Alzheimer's disease. ESAIM: Proc Surv 2020;67:30–45.
[30] Geuzaine C, Remacle J-F. Gmsh: a 3-D finite element mesh generator with built-in pre-and post-processing facilities. Int J Numer Methods Eng 2009;79(11):1309–31.